Journal of Asian Earth Sciences 229 (2022) 105171

Contents lists available at ScienceDirect

Journal of Asian Earth Sciences

journal homepage: www.elsevier.com/locate/jseaes

Tonian and Cryogenian – Early Cambrian sedimentation in NW India: Implications on the transition from Rodinia to Gondwana

Jun Zhang [a], Manoj K. Pandit [b], Wei Terry Chen [c], Wei Wang [a,*]

[a] State Key Laboratory of Geological Processes and Mineral Resources, School of Earth Sciences, China University of Geosciences, Wuhan 430074, China
[b] Department of Geology, University of Rajasthan, Jaipur 302004, India
[c] State Key Laboratory of Ore Deposit Geochemistry, Institute of Geochemistry, Chinese Academy of Sciences, Guiyang 550081, China

ARTICLE INFO

Keywords:
Sedimentary provenance
Sindreth and Punagarh basins
Marwar Supergroup
NW India
Rodinia-Gondwana transition

ABSTRACT

The Tonian Punagarh-Sindreth and Cryogenian – early Cambrian Marwar sequences in NW India encompass a geological record that could provide vital information for working out the tectonic evolution of this region and a better understanding of the Rodinia to Gondwana transition. The Tonian Punagarh and Sindreth sub-basins received a dominantly felsic detritus with negligible sorting of heavy minerals and mild to weak chemical weathering conditions. The clastic compositions and geochemical characteristics of the Punagarh and Sindreth groups suggest a back-arc basin setting and the detritus sourced from a volcanic arc and cratonic interior region. The Punagarh basin was proximal to the craton while the Sindreth basin was close to an arc system. In contrast, the Cryogenian – early Cambrian Marwar Supergroup clastic sequence contains mature quartz arenite whose high CIA (77.8–94.8) and low ICV (0.18–1.00) values suggest a strong chemical weathering in the source region and noteworthy physical sorting during transportation and sedimentation. An abundance of quartz grains (87–94%), enrichment of Zr, and detritus predominantly derived from the cratonic basement indicate deposition of Marwar sediments in a tectonically stable basin, temporally coinciding with the Gondwana assembly. Collectively, the ~ 760 Ma active continental margin in NW India, documented by the provenance and tectonic setting of the Punagarh and Sindreth basins, is in agreement with the subduction of the peripherical Rodinia supercontinent during its breakup. On the other hand, the passive continental margin sedimentation in Marwar Supergroup points toward an open sea between NW India and western Gondwana during the Gondwana assembly.

1. Introduction

The Neoproterozoic Era is hailed as one of the most dynamic periods in Earth's history that also coincides with the transition from Rodinia to Gondwana supercontinents (Hoffman, 1991; Moores, 1991; Li et al., 2008; Evans, 2013; Nance et al., 2014; Wang et al., 2020). Although the Neoproterozoic - Cambrian transition has been evaluated through sedimentary records from different parts of the world (e.g., Cawood et al., 2018; Zhou et al., 2019; Wang et al., 2021a), some potentially significant terranes need further attention for a better understanding of the crustal dynamics during this time interval. The NW peninsular India (hereinafter referred to as the NW India) is one such region where Tonian and Cryogenian – early Cambrian Punagarh-Sindreth groups, and Marwar Supergroup sedimentary sequences hold vital information relevant in unraveling the transition from Rodinia to Gondwana supercontinents, as the Indian continental block drifted from a peripheral location in the Rodinia supercontinent to the central position in the Gondwana assembly (Collins and Pisarevsky, 2005; van Lente et al., 2009; Merdith et al., 2017; Wang et al., 2021a, 2021b). Despite their key position in understanding the middle Neoproterozoic - early Cambrian tectonic evolution of the NW Indian block, the depositional history of these basins continues to be debated on account of diverse and contradictory models (Chore and Mohanty, 1998; Chaudhuri et al., 1999; Roy and Sharma, 1999; Pandey and Bahadur, 2009; van Lente et al., 2009; Dharma Rao et al., 2012; Schöbel et al., 2017).

The Punagarh and Sindreth basins have long been associated with continental extension (Khan and Khan, 2015, 2016; Schöbel et al., 2017; Bhardwaj and Biswal, 2019; Khan et al., 2020), based on sedimentation history and regional deformation geometry. However, it is still unclear whether the driving mechanism was a mantle plume (Bhushan, 2000),

* Corresponding author.
E-mail address: wwz@cug.edu.cn (W. Wang).

https://doi.org/10.1016/j.jseaes.2022.105171
Received 2 November 2021; Received in revised form 16 February 2022; Accepted 26 February 2022
Available online 2 March 2022

faulting-induced half-graben (Schöbel et al., 2017; de Wall et al., 2018), Andean type magmatism (Torsvik et al., 2001b; Ashwal et al., 2002) or a post-orogenic collapse (Bhardwaj and Biswal, 2019). The litho-assemblages in these sub-basins represent an imbricate oceanic plate stratigraphy related to subduction and accretion in a shallow marine depositional environment (Dharma Rao et al., 2012) consistent with an active convergent margin as affirmed by the geochemical characteristics of pillow basalts interlayered with the sediments (van Lente et al., 2009). A back-arc setting for Punagarh and Sindreth basins was postulated by Khan and Khan (2015, 2016) and Khan et al. (2020) who inferred a volcanic arc and craton interior detritus source. These two groups, associated with the Malani (predominantly felsic) magmatism, have been associated with the Neoproterozoic subduction of the Mozambique oceanic crust beneath NW India, Seychelles, and north-eastern Madagascar (Torsvik et al., 2001b; Aswal et al., 2002; Wang et al., 2018c).

Apart from the debated issue of the tectonic setting of Punagarh, Sindreth, and Marwar sequences, their provenances have also been loosely constrained due to limited data (Khan and Khan, 2015, 2016; George and Ray, 2017; Schöbel et al., 2017; Wang et al., 2019; George, 2020; Khan et al., 2020), although the detrital zircon data published during the last decade or so (Malone et al., 2008; Mckenzie et al., 2011; Turner et al., 2014; Wang et al., 2019) have significantly contributed to constraining the sediment source. Petrological and geochemical data of sedimentary rocks have been interpreted in terms of provenance characterization, and paleoweathering and paleoclimatic conditions in the source region, therefore, useful in modeling the 'source to sink' system during the supercontinental cycle (Dharma Rao et al., 2012; Zhao et al., 2020). We have investigated clastic sedimentary rocks from Punagarh, Sindreth, and Marwar basins, and in this paper, we (i) provide constraints on the provenance, (ii) have inferred the tectonic setting of these sedimentary basins, (iii) worked out the middle Neoproterozoic to early Cambrian crustal evolution of NW Indian block, and (iv) implicate upon the transition from Rodinia to Gondwana supercontinental cycles.

2. Geological setting

2.1. Regional geological overview

Peninsular India (Indian Shield) is a collage of five cratonic nuclei, namely the Aravalli, Bundelkhand, Bastar, Singhbhum, and Dharwar cratons, sutured by Proterozoic mobile belts (Naqvi, 2005; Manikyamba et al., 2021). The Aravalli - Bundelkhand cratons, the northernmost ones, are separated from the cratons of the South Indian Block by the almost E-W trending Central Indian Tectonic Zone (CITZ) (Fig. 1). The Aravalli craton in NW Indian shield together with the accreted Marwar Block to its west is separated from the Bundelkhand craton in the east by the Great Boundary Fault. The oldest rock unit in the Aravalli craton is the Banded Gneiss Complex (BGC - Gupta, 1934; Heron, 1953), including 3300–2500 Ma (Gopalan et al., 1990; Wiedenbeck and Goswami, 1994; Roy and Kröner, 1996) BGC-I in the southeast and mainly Paleoproterozoic (Buick et al., 2006; Bhowmik and Dasgupta, 2012)

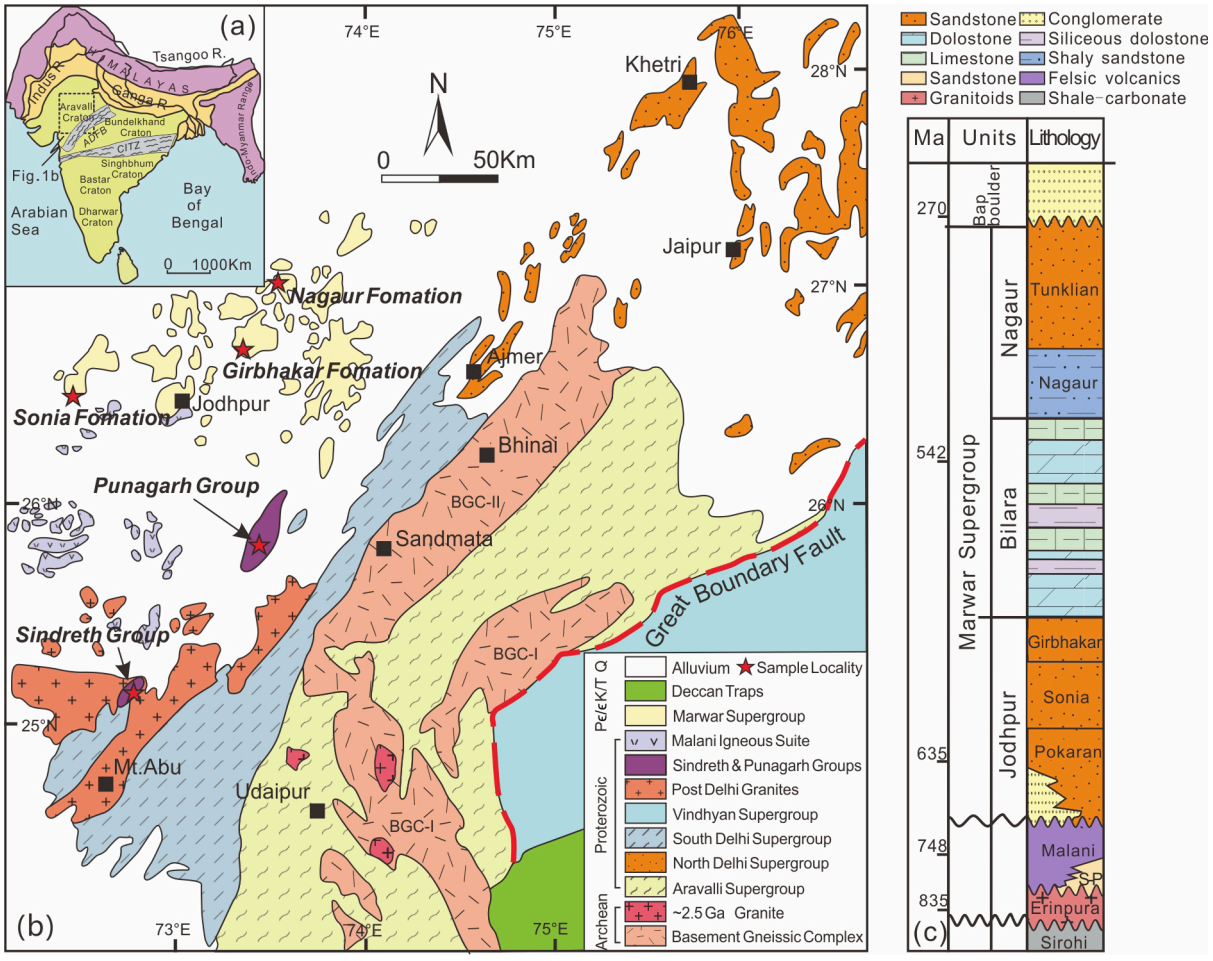

Fig. 1. (a) Framework of Peninsular India (after Roy and Jakhar, 2002); (b) Simplified geological map of the Aravalli craton showing the distribution of major Precambrian geological units of the Aravalli-Delhi Belt (adapted from Roy and Jakhar, 2002; Wang et al., 2018b); (c): Stratigraphic column of middle Neoproterozoic to early Paleozoic successions from northwestern India (adapted from Wang et al., 2019). Abbreviations: ADFB: Aravalli Delhi Fold Belt; CITZ: Central Indian Tectonic Zone; S-P: the Sindreth and Punagarh groups.

BGC-II in the northwest. The former is mainly composed of TTG, gneiss, migmatite, schist, amphibolite, and quartzite (Tobisch et al., 1994; Wiedenbeck and Goswami, 1994; Roy and Kröner, 1996; Kaur et al., 2021), while the latter is subdivided into the Sandmata and Mangalwar complexes, containing high-grade (up to granulite facies) supracrustal rocks, and *meta*-igneous (felsic and basic) rocks (Buick et al., 2006). Unconformably overlying the BCG-I basement are the sediments of Aravalli Supergroup, comprising a mafic volcanic unit intercalated with quartzite and conglomerate in the basal part, followed upward by calcareous and argillaceous sedimentary rocks (Sinha-Roy et al., 1998; Roy and Jakhar, 2002; Wang et al., 2018a, 2018b). The Aravalli Supergroup has been traditionally described a Paleoproterozoic (2500 Ma to 1850 Ma) sequence based on 2500 Ma granitoids in the basement and the 1850 Ma Darwal *syn*-orogenic granite intrusion (Choudhary et al., 1984; Wiedenbeck et al., 1996; Meert et al., 2010). A younger sequence named the Delhi Supergroup, further subdivided into an older North Delhi Group (~1700 Ma) and a younger South Delhi Group (~1000 Ma) (Sinha-Roy, 1984), unconformably overlies the Archean rocks (Heron, 1953; Saini et al., 2006), however, the contact relationship between Aravalli and Delhi supergroups is unclear. The Delhi Supergroup comprises clastic rocks, metasomatic sedimentary rocks, and a small amount of metasomatic volcanic rocks, which have undergone greenschist- to amphibolite-facies metamorphism. Several granitic plutons emplaced within the Aravalli Delhi Fold Belt (ADFB) display two major age groupings, i.e. 1860–1810 Ma and 1720–1660 Ma (Buick et al., 2006; Kaur et al., 2011, 2017; Bhowmik and Dasgupta, 2012; Wang et al., 2017a; Pandit et al., 2021).

The Marwar Block collided with the ADFB at ~ 1000 Ma, as manifested by the occurrence of ophiolite along the Phulad Lineament at the western margin of the Aravalli Delhi Fold Belt (Gupta et al., 1980; Khan et al., 2005, 2019) and the emplacement of the 990–970 Ma calc-alkaline felsic igneous rocks and associated mafic intrusions in the Sendra-Ambaji area (Deb et al., 2001; Pandit et al., 2003). Several granitic plutons emplaced during 1000–800 Ma are collectively referred to as the Erinpura Granite (EG), with major outcrops along the western margin of South Delhi Fold Belt (Coulson 1933; Heron, 1953; Pandit et al., 2003; Purohit et al., 2012). A younger and more extensive suite of magmatic rocks to the west of the Erinpura Granite is designated as the Malani Igneous Suite (MIS) (Pareek, 1981). This predominantly felsic suite of rocks, dated to 770–750 Ma (Torsvik et al., 2001b; Gregory et al., 2009; Meert et al., 2013; Wang et al., 2017b), is the youngest known Precambrian magmatic event in the Marwar Block. The total areal spread of the MIS is about 55000 km^2, most of which is covered by the late Neoproterozoic to early Cambrian Marwar Supergroup and the Quaternary alluvium sediments (Roy and Jakhar, 2002; de Wall et al., 2018).

2.2. *The Punagarh and Sindreth groups*

The Punagarh and Sindreth basins, broadly NNE-SSW trending linear basins along the western margin of the ADFB, are ~ 110 km apart and cover about 150 km^2 and 40 km^2, respectively (Fig. 2). These sedimentary sequences show synclinal folding and significant chemical alteration, however, their pristine textural attributes underline low to insignificant metamorphism (Chore and Mohanty, 1998; Sharma, 2004, 2005; van Lente et al., 2009; Schöbel et al., 2017; de Wall et al., 2018). On account of a similarity in the outcrop patterns, lithological makeup and deformation geometry, and collinear occurrence, the Punagarh and Sindreth sequences are considered coeval litho-units (Chore and Mohanty, 1998; van Lente et al., 2009). The U-Pb geochronological data on the felsic volcanics from Punagarh and Sindreth sequences suggest 769–758 Ma age bracket for sedimentation (van Lente et al., 2009; Wang et al., 2017b, 2018c), synchronous with the 770–750 Ma Malani magmatism (Torsvik et al., 2001b; Gregory et al., 2009; Meert et al., 2013; Wang et al., 2017b; Zhao et al., 2018). These are significantly younger than the Erinpura Granite (800–870 Ma, van Lente et al., 2009; Just et al., 2011) that intrudes the basement rocks of the Sojat Formation and Sirohi Group (Chore and Mohanty, 1998; van Lente et al., 2009; Schöbel et al., 2017). The geochemical characteristics of bimodal volcanic rocks of Sindreth and Punagarh basins suggest their close affinity with Malani

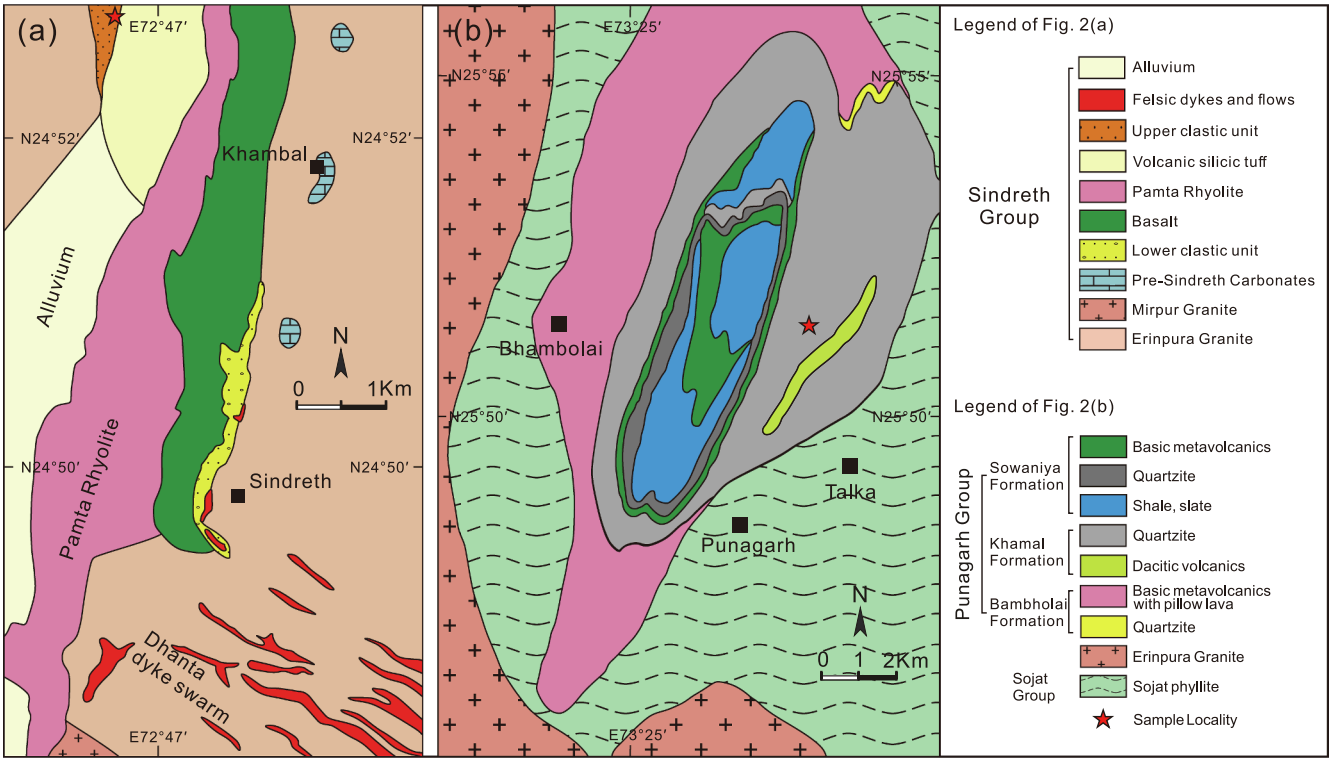

Fig. 2. Geological map showing the distribution of (a) Sindreth and (b) Punagarh volcano-sedimentary sequences, modified from Chore and Mohanty (1998), Sharma (2004), Schöbel et al. (2017), de Wall et al. (2018) and Wang et al. (2018c).

volcanics (van Lente et al., 2009; Dharma Rao et al., 2012; Wang et al., 2018c).

The Punagarh Group is an ~ 4500 m thick sequence (duplicated by folding) that unconformably overlies the Sojat Formation (Chore and Mohanty, 1998; van Lente et al., 2009), and is further subdivided into Bambholai, Khamal, and Sowaniya formations, from oldest to the youngest (Chore and Mohanty, 1998; van Lente et al., 2009). The Bambholai Formation comprises pillow basalt flows interlayered with subordinate shale and quartzite. The Khamal Formation is composed of quartzite and vesicular and amygdaloidal dacitic rocks while Sowaniya Formation comprises repetitive felsic and basic volcanic flows with interlayered quartzite and shale unit at the top (Chore and Mohanty, 1998; van Lente et al., 2009; Khan and Khan, 2015, 2016; Bhardwaj and Biswal, 2019). A subarkose unit of Khamal Formation displaying parallel bedding is well-exposed in a quarry section (Fig. 2b, 4b). Several mafic and felsic dykes crosscut both Sojat Formation and the Punagarh Group rocks (van Lente et al., 2009; Bhardwaj and Biswal, 2019).

The Sindreth Group with a cumulative thickness of ~ 500 m, unconformably overlies Sirohi Group and has been subdivided into Khambal and Angor formations (Chore and Mohanty, 1998). Schöbel et al. (2017) subdivided Sindreth Group into lower clastic (LCU), bimodal volcanic (BVU), and upper clastic (UCU) units, based on mapping carried out in the type section near Sindreth village. The LCU comprises pebbly, coarse-sandstone, and conglomerate while UCU is an ensemble of arkose, conglomerate, lithic greywacke and tuff. The intervening BVU comprises ignimbrite, rhyolite, basalt flows and volcaniclastics (Schöbel et al., 2017). We observed a litharenite interlayer within sandstone (~20 cm thick) and pelitic rocks (~5 cm thick) in the Angor Dam section (Fig. 2a, 4a). The Sindreth and Sirohi groups, together with the basal Erinpura Granite, are crosscut by several WNW to N-S trending dolerite dykes that represent the terminal phase of Malani magmatism in this region (Chore and Mohanty, 1998; Sharma, 2004; van Lente et al., 2009).

2.3. The Marwar Supergroup

The Marwar Supergroup, having a cumulative thickness of > 1000 m (Pareek, 1981), is deposited over the Malani rhyolite over a profound erosional unconformity (Pareek, 1984) (Fig. 4c), and in turn, overlain by the Carboniferous to Permian, Bap Boulder Bed (Chauhan et al., 2001). The Marwar Supergroup, further subdivided into the Jodhpur, Bilara, and Nagaur groups, from oldest to the youngest, comprises a deltaic littoral and shallow marine sequence consisting of sandstones, evaporites, carbonate rocks, and shales (Pareek, 1984) (Fig. 3). The Jodhpur Group represents a fluvial-marine arenaceous sequence with dominant sandstone and minor shale. It is further subdivided into the Pokaran, Sonia, and Girbhakar formations (Pareek, 1984). The Pokaran Formation mainly comprises a basal conglomerate, equivocally considered either an Indian example of the Marinoan tillite (Chauhan et al., 2001) or a fluvial deposit (Cozzi et al., 2012). The Sonia Formation mainly consists of chestnut brown siltstones and shales, white to reddish lenticular sandstones with cross-bedding and ripple marks (Fig. 4d, e), and jasper-dolostone with banded chert (Roy and Jakhar, 2002; Pandey and Bahadur, 2009), suggesting a beach depositional environment (Chauhan et al., 2004). Girbhakar Formation, the youngest unit of the Jodhpur Group, is mainly composed of well-bedded, pisiform, brick-red siltstones, shales, and cross-bedded sandstones (Chauhan et al., 2004) (Fig. 4f). The overlying Bilara Group is a platform carbonate sequence composed mainly of dolostone and stromatolitic limestone. It is subdivided into the Dhanapa (stromatolitic limestones, dolomites, siliceous dolomites), Gotan (limestones with chert and dolomite bands), and Pondlo formations (dolomite, siliceous dolomites, stromatolitic limestones, siliceous oolites) (Pareek, 1984). Pandey and Bahadur (2009) inferred the deposition of Bilara Group in a low to moderately high energy shallow marine basin under a warm and arid climate. Pandit et al. (2001) observed significantly depleted $\delta^{13}C$ values and $\delta^{13}C$

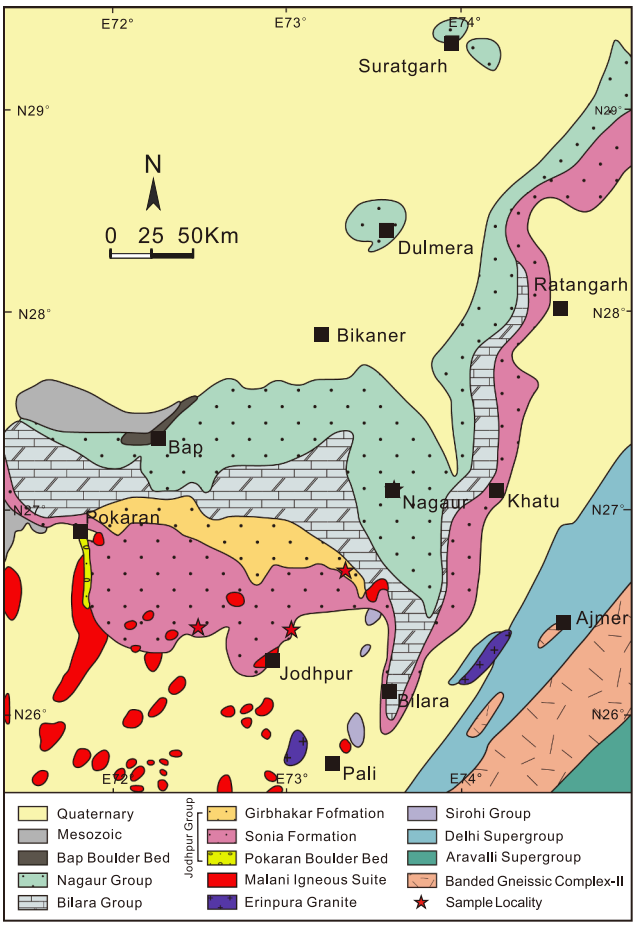

Fig. 3. Geological map showing the distribution of the Marwar Supergroup subdivisions and surrounding litho-tectonic units, modified from Pareek (1984), Roy and Jakhar (2002) and George and Ray (2017).

fluctuations in Bilara Group carbonate rocks that they interpreted to represent the Neoproterozoic – Cambrian transition. The argillaceous - arenaceous facies Nagaur Group unconformably overlies the Bilara Group and has been subdivided into Khichan, Nagaur, and Tunklian formations (Pareek, 1984). The basal conglomerate of the Khichan Formation includes dolomitic and chert pebbles derived from the Bilara Group, representing a sedimentary hiatus (Pandey and Bahadur, 2009). The overlying Nagaur Formation is mainly composed of brick-red sandstones, siltstones, and shales, with greenish clay pockets and evaporites, suggesting a low to high energy marginal sea-to-continental depositional environment with warm and humid climatic conditions. The Tunklian Formation is mainly composed of sandstone, at places pebbly (Pandey and Bahadur, 2009).

A well-defined unconformity between the MIS and Marwar Supergroup fixes the lower age of the Marwar Supergroup at < 750 Ma (Torsvik et al., 2001b; Gregory et al., 2009; Meert et al., 2013; Wang et al., 2017b). The Marwar Supergroup has broadly been assigned an Ediacaran - Cambrian age (McKenzie et al., 2011; George and Ray, 2017), while most of the trace/body fossils lack reliable age control except for the Cambrian trace fossils reported from the Nagaur Group (Kumar and Pandey, 2008, 2010; Singh et al., 2008; Srivastava, 2012). Although, the Marwar Supergroup lacks rock types suitable for geochronology, a small rhyolite/tuff band interlayered with Sonia sandstone of Jodhpur Group at a single location at Chhoti Khatu has yielded 703 ± 40 Ma whole-rock Rb-Sr age (George and Ray, 2017). These ages have a large uncertainty and the whole rock Rb-Sr system is potentially vulnerable to alteration. Therefore, the recently reported 651 ± 18 Ma U-Pb age of the youngest inherited zircon from the same

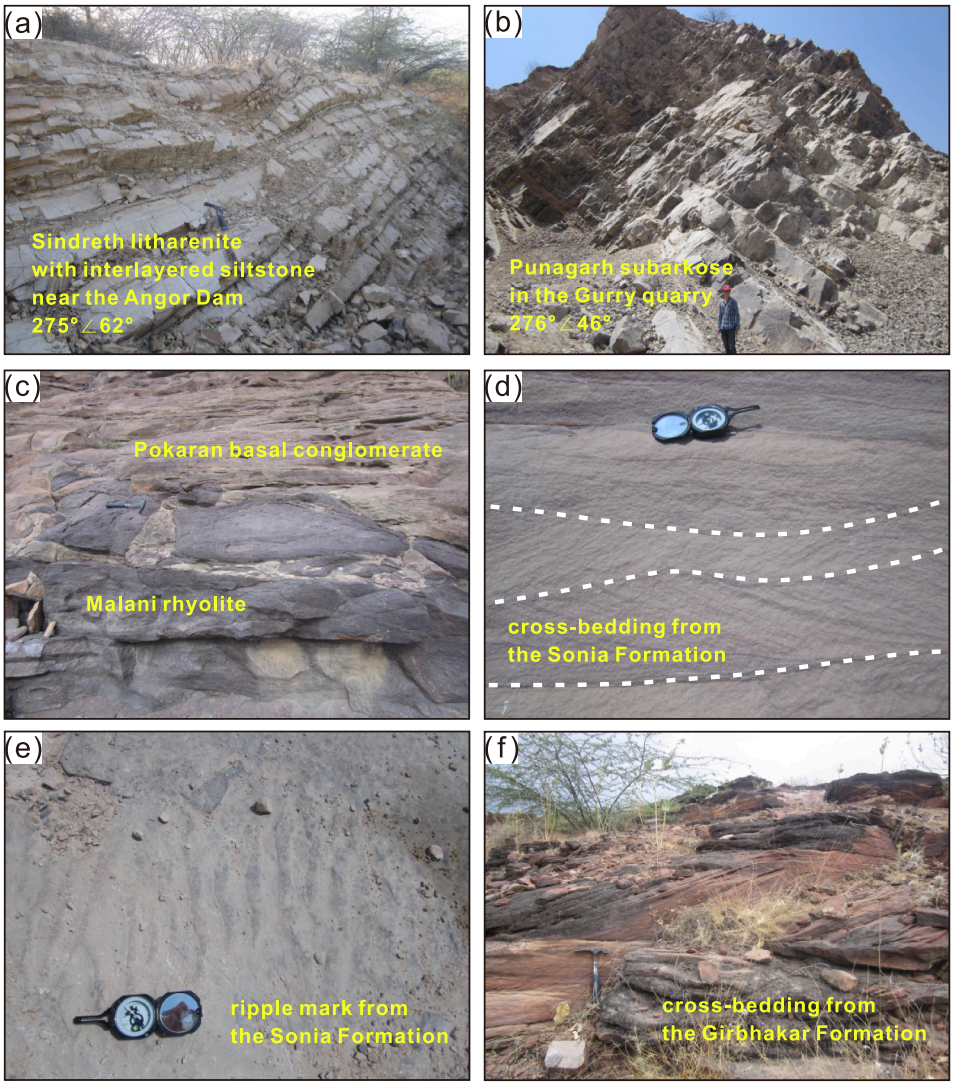

Fig. 4. Field photographs showing (a) fractured grey litharenite from the Sindreth Group; (b) thick layers of grey arkose from the Punagarh Group; (c) unconformity between the Marwar Supergroup sandstone (upper unit) and the Malani rhyolite (lower); (d) cross-bedding and (e) ripple marks in the Sonia Formation sandstone; (f) cross-bedding in the Girbhakar Formation sandstone.

felsic ash layer (Xu et al., 2022) can be considered as the best estimate for a post-Cryogenian initiation of Marwar sedimentation. This assertion is coherent with the proposed < 616 Ma age of Bilara sedimentation, based on detrital zircon U-Pb age (Lan et al., 2020). The stable isotope data on Bilara carbonates indicate Neoproterozoic – Cambrian transition (Pandit et al., 2001; Mazumdar and Bhattacharya, 2004). George and Ray (2017) provided 520–530 Ma and 570 Ma ages for the Gotan Limestone of Bilara Group, based on the $^{87}Sr/^{86}Sr$ isotope data, while George (2021) suggested the depositional age between 539 and 520 Ma. The ca. 540 Ma maximum depositional age of Nagaur sandstone based on the U-Pb detrital zircon data (McKenzie et al. 2011), is consistent with the paleontological evidence for the age of Nagaur Group (Kumar and Pandey, 2008, 2010; Srivastava, 2012).

3. Sampling and analytical methods

Unaltered and fresh representative samples from Punagarh, Sindreth, and Marwar sequences were collected and 36 samples were carefully selected, discarding weathered rinds and veins, for bulk rock geochemistry and Sm-Nd isotope analyses. Sample details are presented in Supplementary Table 1.

3.1. Petrographic characteristics of sandstones

The clastic composition of sandstone was calculated with the point-counting method (Dickinson, 1985) using a polarizing microscope. The following parameters were noted for the statistical analysis. The total number of quartz grains (Qt) including monocrystalline (Qm) and polycrystalline quartz (Qp); the total number of feldspar particles (F) including plagioclase (Pl) and K-feldspar (Kf); the total number of unstable rock fragments (L) including igneous (Lv), sedimentary (Ls) and metamorphic (Lm) rock debris.

3.2. Bulk rock major and trace elements

Although only alteration-free, fresh samples were selected for geochemistry, the rind of each sample was discarded during preparation and only the central part (>200 g) was cleaned, dried, and pulverized to ~ 200 mesh in an agate mill. Major elements were analyzed by an X-ray fluorescence spectrophotometer (XRF), at the State Key Laboratory of Geological Processes and Mineral Resources, China University of Geosciences, Wuhan. International standards (GSR-1, GSR-3) were employed for calibration, and observed analytical precision was usually better than 5%. Trace and Rare Earth Element analyses were performed

by an Agilent 7500a ICP-MS at the State Key Laboratory of Geological Process and Mineral Resources, China University of Geosciences, Wuhan. About 50 mg sample powder was moistened with a few drops of ultrapure water and digested in a mixture of 1.5 ml HF + 1.5 ml HNO_3 in a sealed Teflon crucible and kept in an oven at 190 °C for 48 h to ensure complete digestion. The digested sample was evaporated to dryness at ~ 115 °C, and 1 ml HNO_3 was added before the second cycle of evaporation to dryness. The residue (salt) was dissolved in ~ 3 ml of 30% HNO_3 and resealed and heated in a Teflon bomb at 190 °C for 12 to 24 h. The final solution was diluted to ~ 100 ml by adding 2% HNO_3 before ICP-MS analysis. International standards, BHVO-2, AGV-2, W-2, GSP-2, were used throughout the analytical procedure. The results reveal analytical precision better than 5% for elemental concentrations higher than 10 ppm, and ~ 10% for those with < 10 ppm concentration.

3.3. Nd isotopic analysis

The Sm-Nd isotopic analyses were carried out at the Nanjing FocuMS Technology Co. Ltd, using a Multi-Collector-Inductively Coupled Plasma Mass Spectrometer (MC-ICP-MS). Approximately ~ 100 mg powder was mixed with 0.5 ml of 60 wt% HNO_3 and 1.0 ml 40 wt% HF in high-pressure PTFE bomb. The bomb was steel-jacketed and placed in the oven at 195 °C for 3 days. The digested sample was dried on a hotplate and the residue was dissolved in 1.5 ml of 1.5 N HCl before ion exchange purification. The separation and purification of Sm and Nd were performed following the HDEHP method. The measured $^{143}Nd/^{144}Nd$ ratios were normalized to $^{146}Nd/^{144}Nd = 0.721900$. The USGS geochemical standards, BCR-2, BHVO-2, AVG-2, RGM-2 were used for quality control. The measured isotopic results agreed with the recommended values, within acceptable analytical uncertainty (Weis et al., 2006).

4. Results

4.1. Sandstone petrography

The composition of clastic components of studied sandstone samples is presented in Supplementary Table 2. All the Punagarh samples have grains ranging from 0.1 to 0.3 mm, occasional ones measuring up to 0.5 to 0.6 mm, and are classified as subarkose (Fig. 5b, 6). They comprise moderately sorted sub-rounded minerals and grain-supported framework, while textural attributes indicate a moderate grain maturity. The minerals include predominant quartz (83–86%) and minor proportions of feldspar (6–9%) and lithic fragments (6–8%). Quartz grains are mainly monocrystalline with visible cracks while feldspar grains are

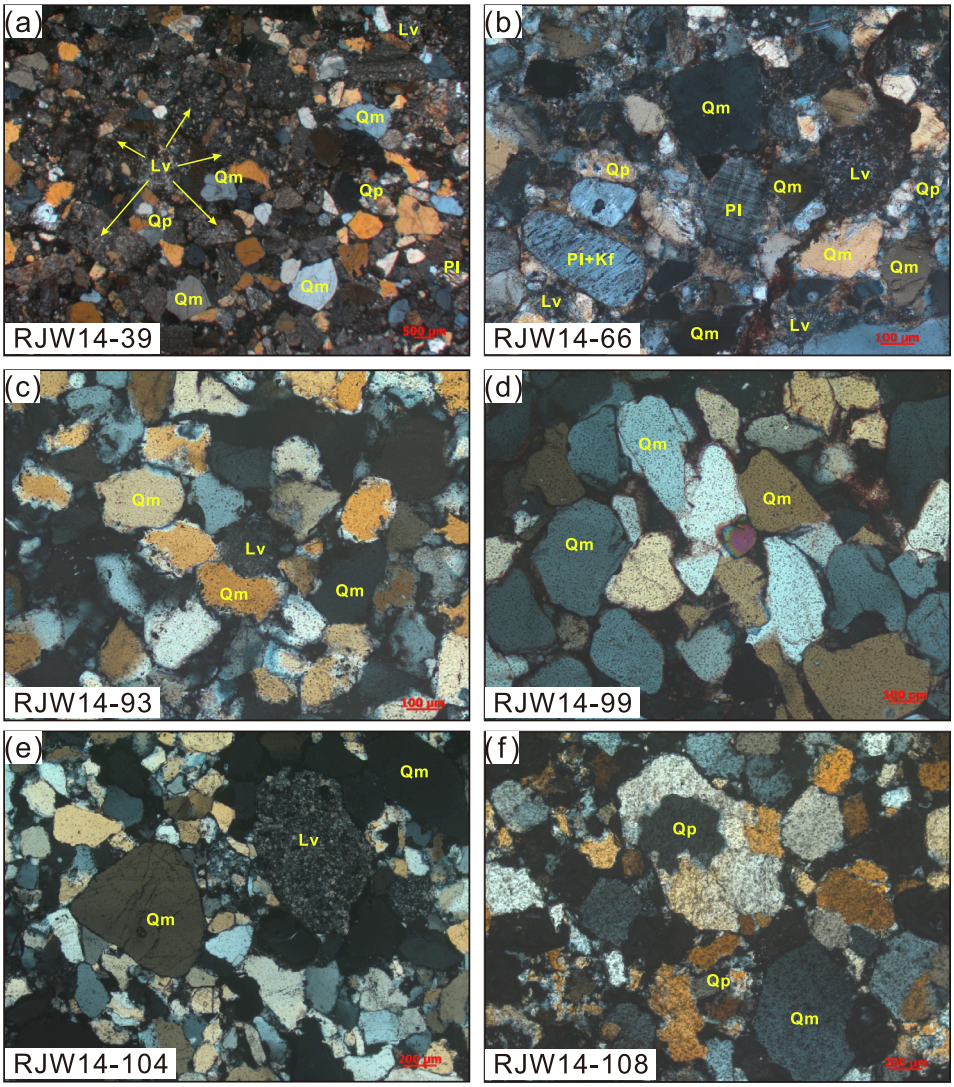

Fig. 5. Photomicrographs of selected sandstones showing detrital components. (a) Sindreth litharenite RJW14-39; (b) Punagarh subarkose RJW14-66; (c) Sonia quartz arenite RJW14-93; (d) Girbhakar quartz arenite RJW14-99; (e) Nagaur quartz arenite RJW14-104; (f) Nagaur quartz arenite RJW14-108. (Ls, sedimentary-lithic grain; Lm, metamorphic-lithic grain; Lv, volcanic-lithic grain; Qm, monocrystalline quartz; Qp, polycrystalline quartz; Kf, K feldspar; Pl, plagioclase).

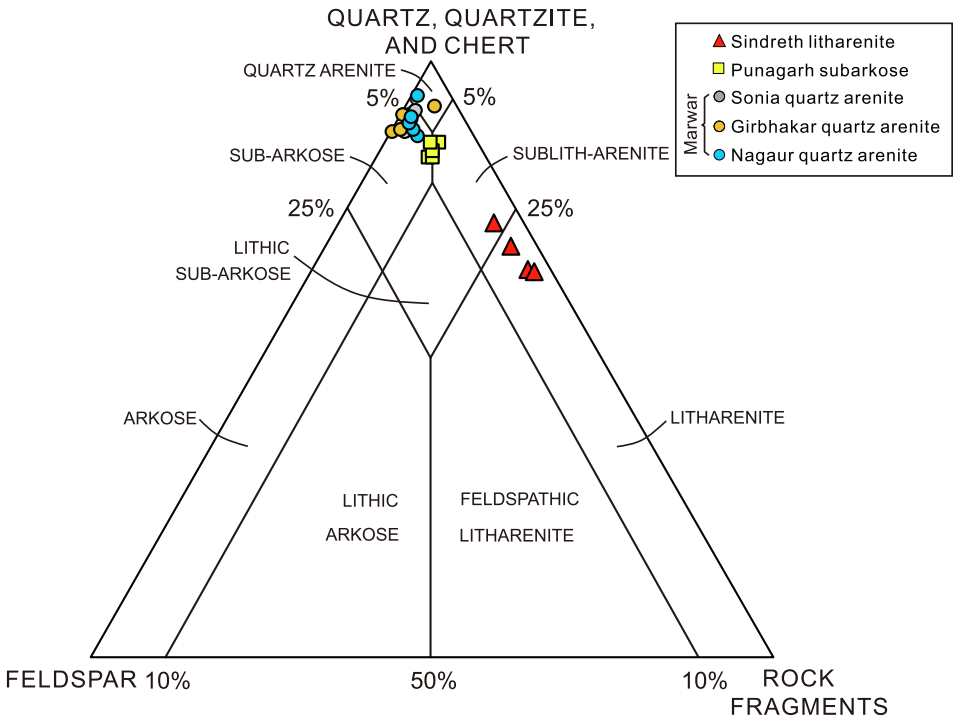

Fig. 6. Classification diagram of common sandstones from Sindreth, Punagarh, and Marwar sequences (after Mcbride, 1963).

partially altered. The lithic fragments are mainly argillaceous rocks and chert.

The Sindreth samples are texturally immature, as indicated by their moderately to poorly sorted nature and sub-angular to sub-rounded grain morphologies, and grain-support framework, typical of litharenite. The size of clastic grains in these samples varies from 0.2 mm to 0.5 mm, with a few larger (up to 1 mm) lithic fragments (Fig. 5a). Monocrystalline and polycrystalline quartz (64–73%) is the major component besides lithic fragments (22–32%) and minor feldspar (3–5%). Quartz grains often display cracks, while feldspar grains are weathered and altered, and display perthitic, vermicular, and graphic intergrowth texture. The lithic fragments are mainly volcanic rocks, chert, and mudstone.

The Marwar sandstones display a high textural grain maturity and are distinct from Punagarh and Sindreth samples, as indicated by their moderate to well-sorted and rounded to sub-rounded grain-supported features. Most clastic grains in Marwar quartz arenite (sandstone) are between 0.1 and 0.3 mm. They have predominant monocrystalline quartz (87–94%), minor feldspar (4–12%), and lithic fragments (0–4%). The Sonia and Girbhakar formation sandstone samples are generally devoid of lithic fragments (Fig. 5c, d), while lithic fragments and polycrystalline quartz are present in Nagaur Group samples (Fig. 5e, f).

4.2. Bulk rock geochemistry

Major and trace element contents of analyzed samples are shown in Supplementary Table 3. Samples from the Sindreth Group have the lowest SiO_2 (77.0–83.4 wt%) and the highest Fe_2O_3 (1.50–3.19 wt%), Na_2O (2.57–4.25 wt%), MgO (0.26–0.66 wt%), and CaO (0.12–1.48 wt %) contents among the total dataset. On the other hand, the Marwar quartz arenites have the highest SiO_2 (88.4–97.5 wt%) and the lowest Fe_2O_3 (0.03–1.46 wt%), Al_2O_3 (1.38–6.17 wt%), Na_2O (0.04–0.11 wt%), K_2O (0.04–0.43 wt%), MgO (0.10–0.29 wt%) and CaO (0.02–0.28 wt%) contents. The Punagarh subarkose samples display intermediate compositions, e.g., 85.4–90.9 wt% SiO_2, 4.75–6.89 wt% Al_2O_3, 0.32–1.19 wt % Fe_2O_3, 0.32–0.51 wt% MgO, 0.10–0.18 wt% CaO, 0.62–1.03 wt% Na_2O and 2.27–2.92 wt% K_2O. The Sonia shales from the Marwar Supergroup have the highest Al_2O_3 (10.59–15.90 wt%) and K_2O (3.70–4.23 wt%) contents.

Sindreth and Punagarh samples have moderately large ion lithophile elements (LILE) contents, such as Rb (67.7 and 86.4 ppm), Sr (57.1 and 30.7 ppm), Th (12.6 and 7.11 ppm), U (1.99 and 1.47 ppm) average contents, respectively. They display moderate abundances of high field strength elements (HFSE), such as Zr (155 and 272 ppm), Hf (4.19 and 6.96 ppm), Nb (7.74 and 3.75 ppm), Ta (0.87 and 0.47 ppm) average contents, respectively. Conversely, the Marwar quartz arenites have distinctively lower LILE contents with the lowest Rb (1.32–9.02 ppm), Sr (5.72–53.6 ppm), Th (2.62–20.9 ppm), and U (0.46–3.79 ppm) abundances, and variable Zr (76–813 ppm), Hf (1.81–20.79 ppm), Nb (0.33–19.7 ppm) and Ta (0.04–2.25 ppm) contents. In the UCC normalized multi-element spider diagrams, they display distinct positive Zr and Hf anomalies, and negative Nb and Ta anomalies as compared to Sindreth and the Punagarh samples (Fig. 7). The Sonia shales are significantly enriched in LILE (e.g., Rb 139–189 ppm, Sr 248–320 ppm, Th 15.2–23.9 ppm, U 1.64–4.11 ppm) and HFSE (e.g., Zr 232–398 ppm, Hf 6.26–10.9 ppm, Nb 12.1–19.6 ppm, Ta 1.37–2.25 ppm), as well as in transitional elements (e.g., Sc 9.37–14.0 ppm, V 56.9–76.6 ppm, Ni 26.1–32.3 ppm), relative to the Marwar quartz arenites.

Despite a large variation in the absolute REE concentrations, all the samples display similar chondrite-normalized REE patterns (Fig. 8). The Marwar quartz arenites and the Punagarh subarkose have low ΣREE (avg. 59.1 and 76.6 ppm, respectively), and display highly fractionated REE patterns (avg. $(La/Yb)n = 8.97$ and 9.41, respectively) with moderately negative Eu anomalies (avg. $Eu/Eu^* = 0.55$ and 0.69, respectively). The Sindreth litharenites and the Sonia shales have slightly higher ΣREE (avg. 142 and 201 ppm), lower (La/Yb)n (avg. 8.30 and 5.78, respectively), and lower Eu/Eu* (avg. 0.58 and 0.54, respectively) as compared to the rest of the data.

4.3. Sm-Nd isotopes

Sm-Nd isotopic ratios of analyzed samples are presented in Supplementary Table 4. The Punagarh samples have initial $^{143}Nd/^{144}Nd$ ratios ranging from 0.510889 to 0.510911, εNd(t) from −15.0 to −14.6, and

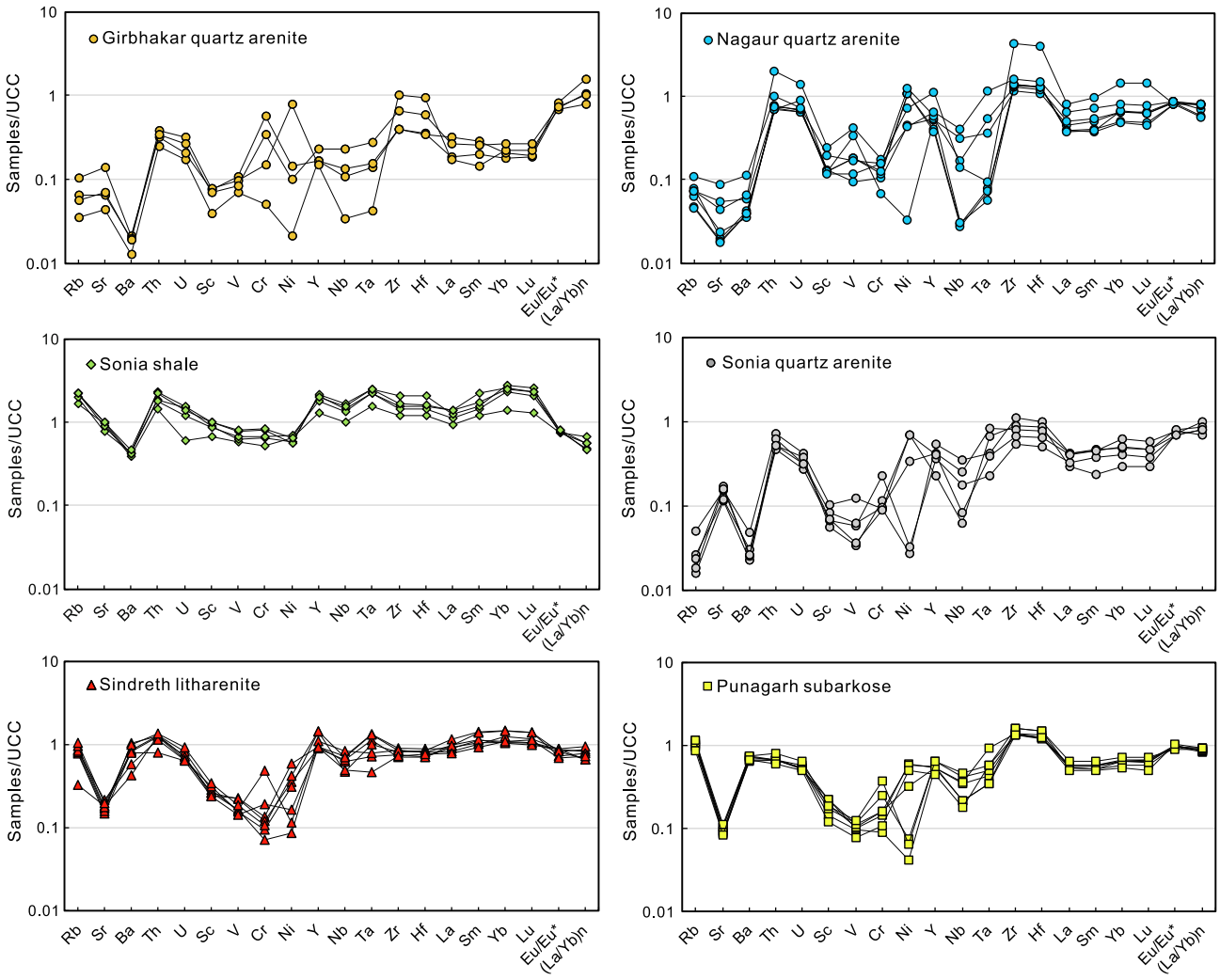

Fig. 7. Average Upper Continental Crust (UCC) normalized multielement spider diagrams of Sindreth, Punagarh, and Marwar samples. Normalizing values of UCC are from Taylor and McLennan (1985).

T_{DM2} from 2650 Ma to 2616 Ma. The Sindreth samples have initial $^{143}Nd/^{144}Nd$ ratios ranging from 0.511565 to 0.511681, εNd(t) from −1.81 to + 0.46, and T_{DM2} from 1584 Ma to 1401 Ma. The Marwar samples have variable initial $^{143}Nd/^{144}Nd$ ratios that range from 0.511079 to 0.511374, εNd(t) from −14.1 to −9.8, and T_{DM2} from 2486 Ma to 2136 Ma.

5. Discussion

5.1. Provenance of the Punagarh, Sindreth, and Marwar basin sediments

5.1.1. Heavy mineral sorting

Elements, such as Al, Fe, Ti, Th, Sc, Co, and La, are considered relatively immobile during post-sedimentation and later processes, and have a low residence time in the water, therefore, useful in deciphering the provenance and tectonic setting (Taylor and McLennan, 1985; Bhatia and Crook, 1986). In the Fe_2O_3, TiO_2 and Al_2O_3 binary plots (Fig. 9a, b), samples from each group demonstrate a generally linear array, indicating similar hydrodynamic behavior during physical sorting and immobility of these elements during chemical weathering (Fralick and Kronberg, 1997).

In the Th/Sc vs. Zr/Sc diagram, the Sindreth litharenites and Sonia shales define a distinct trend, implying that the first-cycle source rocks were unaffected by sedimentary sorting and/or recycling (Fig. 10a). The Punagarh and Marwar samples do not show any zircon addition trend despite their high Zr/Sc ratios (Fig. 10a). The lack of a notable negative correlation between (La/Yb)n and Zr in Sindreth, Punagarh, and Marwar sandstones (Fig. 9c) further suggests a negligible influence of zircon sorting on Zr and REE concentrations. Further, a lack of positive correlation between (La/Yb)n and P_2O_5 (Fig. 9d) indicates insignificant monazite and apatite sorting. Therefore, the HREE enrichment can be regarded as a source-inherited feature rather than resulting from the sorting of zircon and phosphate bearing minerals. This implies that sorting of heavy minerals did not have any significant influence on the chemical composition and geochemical traits reflect the source characteristics.

5.1.2. Provenance characterization

The Punagarh subarkose samples have relatively lower La/Th ratios and moderate Hf contents, suggesting a mixed source comprising old components of passive margin and felsic materials from an arc-setting (Fig. 10b). Their low Sc/Th and moderate La/Sc ratios further suggest a dominantly felsic source (Fig. 10c), consistent with the inference drawn from the Eu/Eu* vs. (La/Yb)n diagram (Fig. 10d). Their non-radiogenic Nd isotopic signatures (εNd(t) = -15.0 to −14.6) further imply a dominant contribution from old and felsic rocks in the sedimentary detritus source (Fig. 11). The geochemical characteristics of Sindreth samples indicate derivation from acidic sources (Fig. 10b, c, d), arguing for a felsic provenance with a lesser recycled component. The Sindreth samples have relatively higher εNd(t) values (-1.81 to + 0.46),

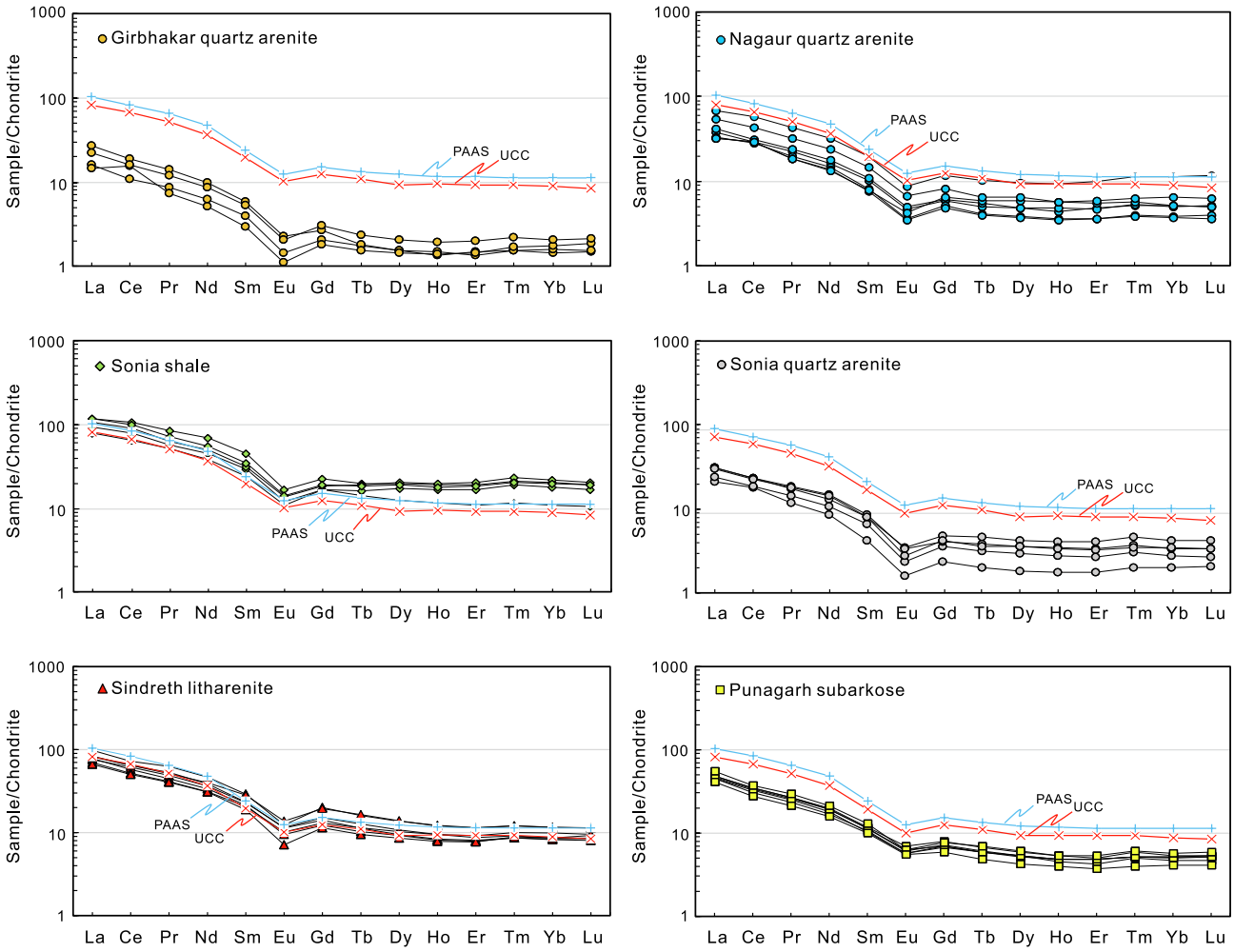

Fig. 8. Chondrite normalized REE patterns of Sindreth, Punagarh, and Marwar samples. Normalizing values of Chondrite, UCC and PAAS are from Taylor and McLennan (1985).

suggesting a dominant juvenile and felsic component in the source (Fig. 11).

The Marwar samples have low La/Th ratios and variable Hf contents that suggest contribution from a mixed source comprising older components from a passive margin and felsic material from arc-related sources (Floyd and Leveridge, 1987) (Fig. 10b), similar to the Punagarh subarkose samples. Their high La/Sc ratios point toward a dominant supply of mature detritus sourced from a passive margin (Fig. 10c) while a wide range of (La/Yb)n and Eu/Eu* values further indicate felsic components in the source (Fig. 10d). Similar to Punagarh subarkose, the Nd isotope compositions (εNd(t) = -14.1 to -9.8) of Marwar samples further argue for old and felsic rocks in the source (Fig. 11). Relatively higher Sc/Th and lower La/Sc ratios of the Sonia shales indicate enrichment of Sc relative to REE and Th in the fine-grained sediments (Fig. 10c).

All the geochemical and isotopic characteristics discussed above converge toward a relatively juvenile and felsic source for Sindreth Group detritus, while the coeval Punagarh Group received a dominant detritus supply from the old and felsic source. The Marwar Supergroup sediments were derived from diverse sources, comprising a dominant old component from a passive margin setting and felsic rocks from arc-related sources.

5.1.3. Source rocks for Punagarh, Sindreth, and Marwar sediments

Neoarchean to Proterozoic multiple sources for Punagarh, Sindreth, and Marwar sedimentary rocks were inferred in the earlier studies (Khan and Khan, 2015, 2016; George and Ray, 2017; Schöbel et al., 2017; Wang et al., 2019; George, 2020; Khan et al., 2020). We have compiled a total of 884 detrital zircon U-Pb age data from the published works to evaluate the provenance information. The detrital zircon data are provided in Supplementary Table 5 and exhibited in Fig. 12. Common provenance characteristics for the Punagarh, Sindreth, and Marwar sediments are discernible in the diagram albeit with a variable contribution from the individual source. These zircon age peaks correlate well with the known magmatic events in the ADFB: (a) Neoproterozoic zircons with age peaks at ~ 760 Ma and ~ 820 Ma were derived from the Malani igneous suite (770–750 Ma) (Torsvik et al., 2001b; Gregory et al., 2009; Meert et al., 2013; Wang et al., 2017b; Zhao et al., 2018) and Erinpura Granite (870–800 Ma) (Deb et al., 2001; van Lente et al., 2009; Just et al., 2011), respectively; (b) Mesoproterozoic zircons with an age peak at ~ 1000 Ma may be related to the Sendra calc-alkaline granite of the Delhi Supergroup (1000 Ma) (Deb et al., 2001; Pandit et al., 2003; Zhao et al., 2018); (c) Paleoproterozoic zircons with an age peak at ~ 1800 Ma may be related to the ~ 1850 Ma Darwal Granite, ~1700 Ma BGC-II and/or extensional magmatic rocks of North Delhi Fold Belt (Choudhary et al., 1984; Biju-Sekhar et al., 2003; Buick et al., 2006; Bhowmik and Dasgupta, 2012; Dharma Rao et al., 2013; Kaur et al., 2013; Turner et al., 2014; Pandit et al., 2021); (d) Archean zircons with age peaks at ~ 2500 Ma and ~ 3200 Ma match well with the Berach Granite and BGC-I basement, respectively (Gopalan et al., 1990; Wiedenbeck and Goswami, 1994; Roy and Kröner, 1996; Wiedenbeck et al., 1996).

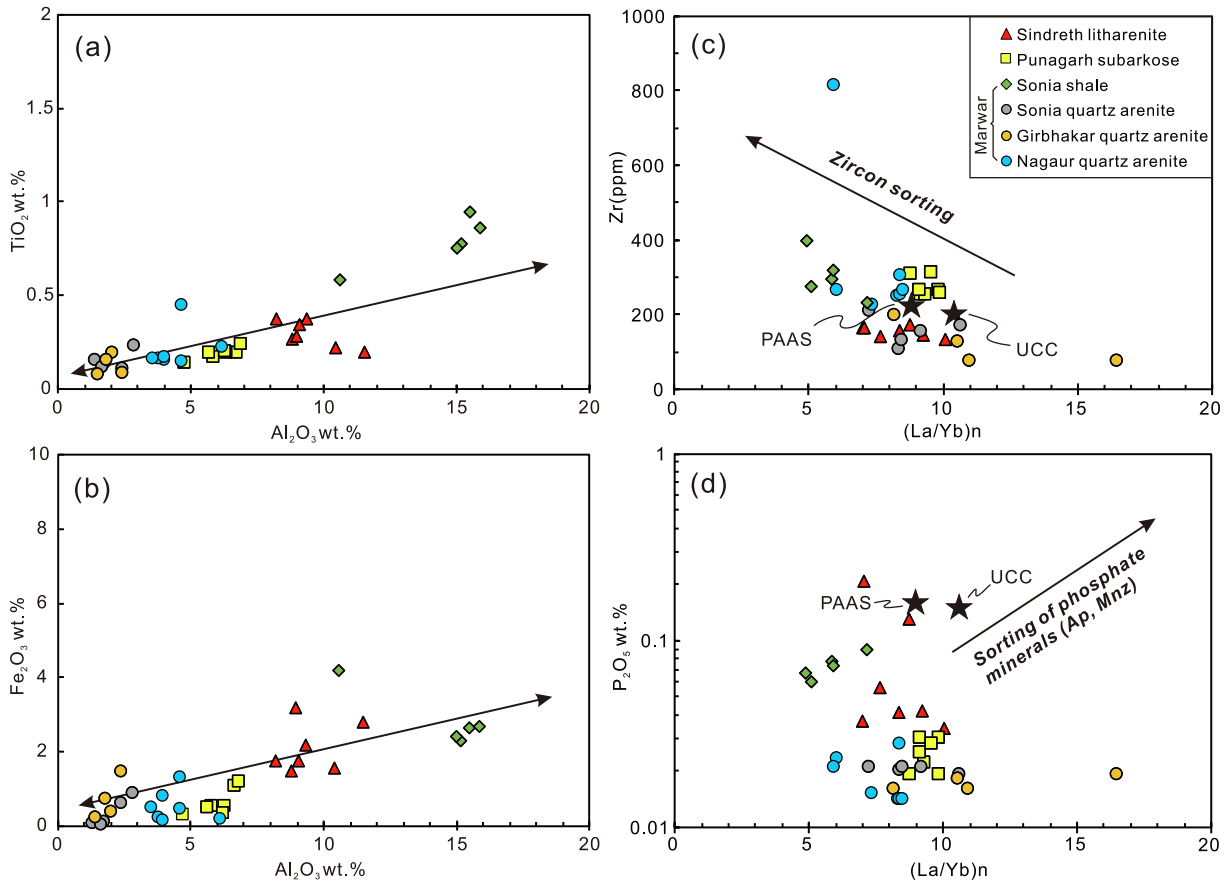

Fig. 9. Binary plots showing the correlation between (a) Al_2O_3 and TiO_2, (b) Al_2O_3 and Fe_2O_3, (c) (La/Yb)n and Zr, (d) (La/Yb)n and P_2O_5 pairs for the Sindreth, Punagarh, and Marwar samples. The compositions of PAAS (Post Archean Australia Shale, Taylor and McLennan, 1985) and UCC (Upper Continental Crust, Taylor and McLennan, 1985) are also plotted for comparison. Ap: apatite; Mnz: monazite.

The Punagarh detrital zircons display a prominent peak at ~ 2510 Ma and two minor peaks at ~ 950 Ma and ~ 1600 Ma (Fig. 12), indicating dominant contributions from BGC-I and Berach Granite sources and limited contribution from the Neoproterozoic magmatic rocks of the Aravalli craton. The Punagarh rocks are feldspar-rich (Fig. 5c), possibly derived from the regional tectonic uplift of a nearby granitic source area. The dominance of sub-rounded to sub-angular grains and other textural characteristics of the Punagarh samples also point toward a proximal source. All the aforesaid observations suggest that Punagarh Group rocks received detritus from the uplifted basement rocks of the BGC-I and the Berach Granite, with the detritus experiencing small-distance transportation and poor sorting.

The Sindreth detrital zircons display a prominent age peak at ~ 830 Ma and two minor peaks at ~ 1780 Ma and ~ 2520 Ma (Fig. 12), indicating major input from Neoproterozoic magmatic rocks (770–750 Ma MIS and 870–800 Ma Erinpura Granite), quite distinct from the Punagarh Group with major detrital flux sourced from the Neoarchean - Paleoproterozoic basement. The Sindreth litharenites show grain immaturity and contain felsic volcanic lithic fragments (Fig. 5a), suggesting a proximal source with wide-spread volcanic rocks. This implies that the Sindreth sediments were sourced mainly from the Malani volcanic rocks of the Marwar Block with subordinate contributions from the ~ 1850 Ma Darwal Granite, ~1700 Ma BGC-II, and ~ 2500 Ma Berach Granite in the Aravalli Craton. Our zircon age distribution patterns are in contradiction to Khan and Khan (2015, 2016) and Khan et al. (2020) who proposed that both Punagarh and Sindreth groups received detritus from the Mesoproterozoic Delhi arc.

Detrital zircons from different stratigraphic units of the Marwar Supergroup display similar zircon age patterns that can be resolved into three obvious age groupings, i.e. 700 Ma to 900 Ma (peaks at ~ 760 Ma and ~ 820 Ma), 1700 Ma to 1900 Ma (single peak at ~ 1800 Ma) and 2450 Ma to 2550 Ma (single peak at ~ 2500 Ma), and two subordinate age groups with peaks at 1000 Ma and 3200 Ma (Fig. 12). Deposition in the Marwar basin was accompanied by a continuous increase in the proportion of young detrital zircons (McKenzie et al., 2011). The euhedral to subhedral shapes of Neoproterozoic zircons (Wang et al., 2019) and the presence of lithic fragments and polycrystalline quartz (Fig. 5e, f) in Nagaur Formation sandstones indicate a proximal source. Based on the geochemistry of siliciclastic sediments, George and Ray (2017) suggested that the contribution of MIS was restricted to the lower unit of the Marwar Supergroup. The detrital zircon age distribution shows that the 770–750 Ma MIS may have provided the clastic detritus to the Nagaur Formation, significantly higher than the underlying Sonia and Girbhakar formations of the Jodhpur Group. A striking feature of the Marwar zircon age patterns is the increasing contribution from ~ 2500 Ma Berach Granite and ~ 3200 Ma BGC-I basement. Besides a dominant Neoproterozoic detritus, the Marwar Supergroup rocks have a significant Paleoproterozoic zircon population that can be related to the ~ 1850 Ma Darwal Granite and ~ 1700 Ma BGC-II in the ADFB. The Hf isotopic data also show a remarkable resemblance between 1800 and 1700 Ma detrital zircons and the BGC-II (Turner et al., 2014). East-to-west paleocurrent directions determined from cross-bedding and ripple marks in the Marwar sandstones also suggest that the Marwar sediments were mainly sourced from the ADFB in the east (Chauhan and Ram, 1999; Wang et al., 2019). A high degree of textural and compositional maturity and well-sorted sediments of the Marwar sandstones underline a long-distance transport and derivation from old rocks exposed in the ADFB and further east. These conclusions are consistent

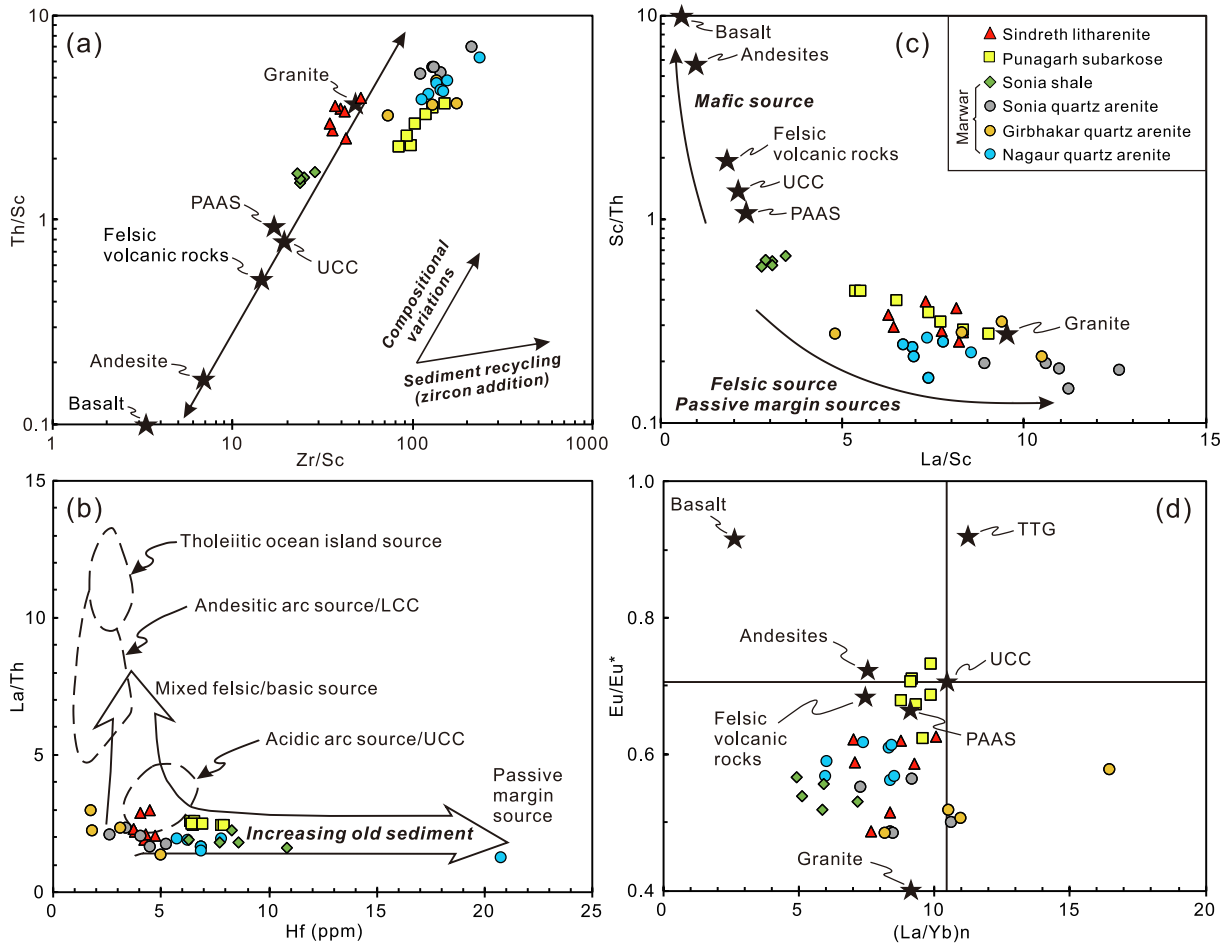

Fig. 10. Binary plots showing the correlation between (a) Th/Sc and Zr/Sc, (b) La/Th and Hf, (c) Sc/Th and La/Sc, (d) Eu/Eu* and (La/Yb)n for the Sindreth, Punagarh, and Marwar samples, along with UCC and PAAS from Taylor and McLennan (1985) and average Proterozoic felsic volcanic rocks, andesite, basalt, granite and TTG from Condie (1993).

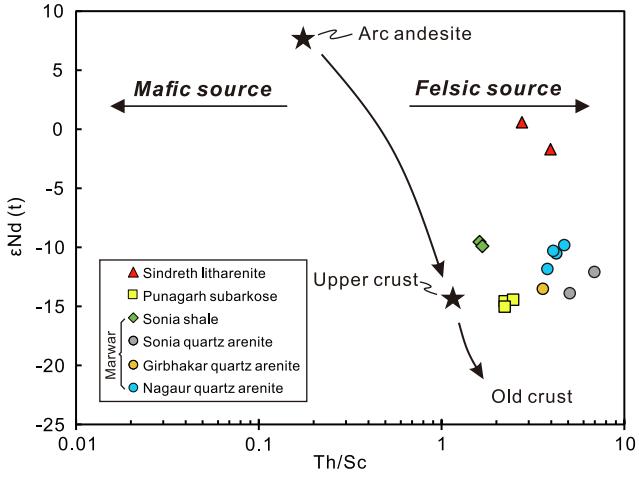

Fig. 11. Nd isotopic compositions and trace element characteristics of Sindreth, Punagarh, and Marwar samples. Arrows indicate general mixing trends (after McLennan et al., 1993). For Nd-isotopic calculations t = 760 Ma (van Lente et al., 2009; Wang et al., 2017b, 2018c) is applied as the depositional age of Punagarh and Sindreth groups for the Nd isotopic calculation; t = 650 Ma (Xu et al., 2022) for the Sonia and Girbhakar formations and t = 540 Ma (McKenzie et al., 2011) for the Nagaur Formation.

with George and Ray (2017) that these sediments were derived from local sources located along the eastern margin of the Marwar basin.

5.2. Middle Neoproterozoic to early Cambrian paleoweathering conditions in NW India

5.2.1. The Punagarh and Sindreth basins

The Chemical Index of Alteration (CIA) is a popular method for estimating the degree of weathering in the source region (Nesbitt and Young, 1982). Besides, the Index of Compositional Variability (ICV) can discriminate between the first cycled (high ICV value) and recycled (low ICV value) sediments (Cox et al., 1995). In the A-CN-K diagram, the Punagarh samples plot as a single cluster (Fig. 13a), indicating well-preserved primary signatures and insignificant effect of diagenesis and post-depositional K-metasomatism. Their ICV (0.76–0.83) and CIA (59.4–62.2) values are lower than the Post Archean Australian Shale (PAAS – 74; Taylor and McLennan, 1985), suggesting weak to mild weathering in the source area (Fig. 13b).

The Sindreth samples display an evolutionary trend towards the K apex in the A-CN-K diagram (line 2 of Fig. 13a), indicating post-depositional K-metasomatism, representing replacement of plagioclase by K-feldspar. Therefore, the CIA values may not change significantly due to the constant sum of Ca + Na + K in feldspar. The CIA values of Sindreth samples range from 53.1 to 58.2 that are significantly lower than PAAS (74), indicating an insignificant weathering effect in the source area (Fig. 13b). Their ICV values range between 0.80 and 1.04, suggesting compositional immaturity for Sindreth samples and the

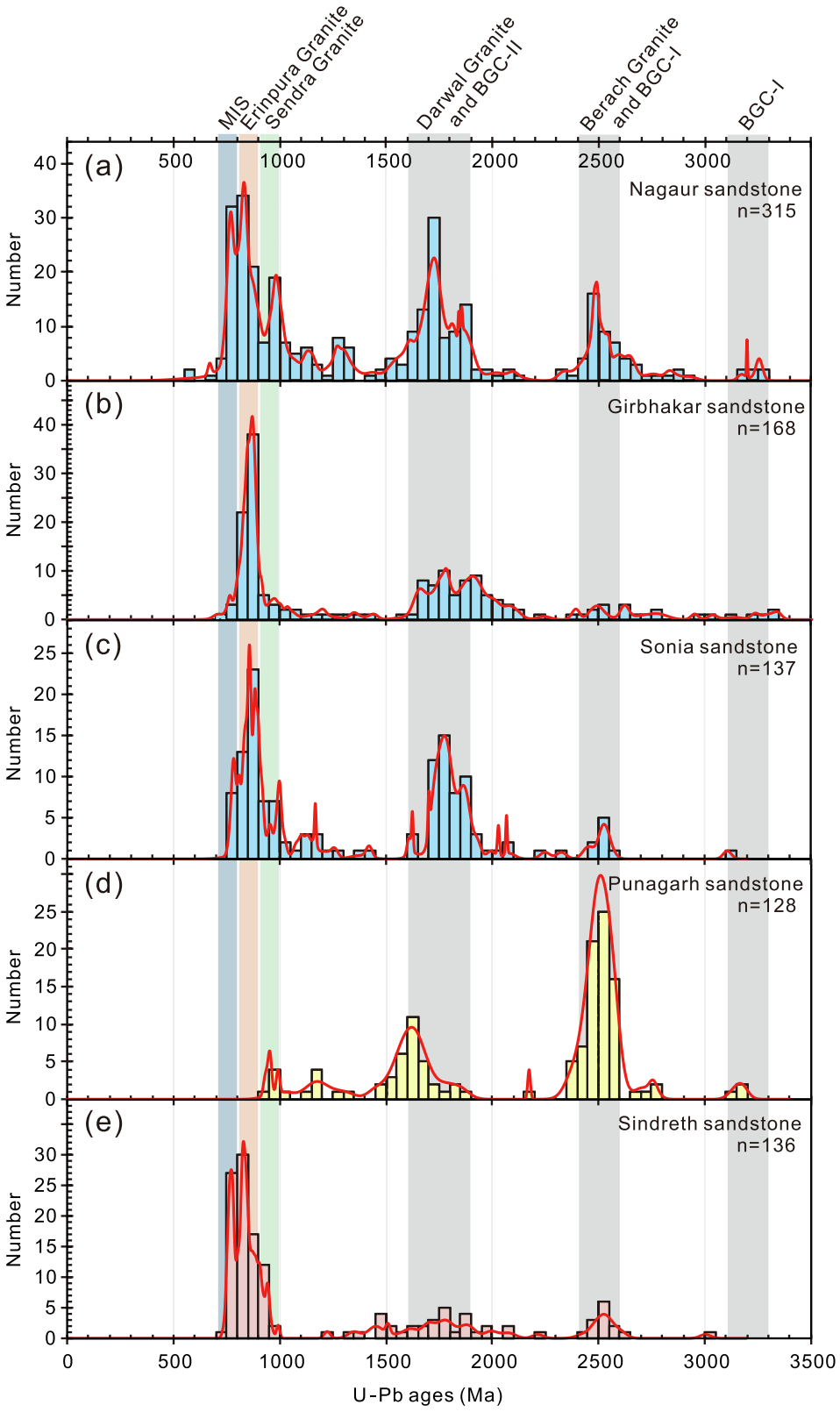

Fig. 12. Detrital zircon age distributions of studied sedimentary rocks. (a) Nagaur sandstone, n = 315 (135 from Mckenzie et al., 2011; 21 from Turner et al., 2014; 159 from Wang et al., 2019); (b) Girbhakar sandstone, n = 168 (72 from Malone et al., 2008; 96 from Wang et al., 2019); (c) Sonia sandstone, n = 137 (43 from Malone et al., 2008; 94 from Wang et al., 2019); (d) Punagarh sandstone, n = 128 (all from Wang et al., 2019); (e) Sindreth sandstone, n = 136 (all from Wang et al., 2019). A complete list of data and data sources is given in the Supplementary Table 5.

detritus derived from the first-cycle source, consistent with their unimodal (Neoproterozoic) detrital zircon age distribution (Fig. 12).

5.2.2. *The Marwar basin*

Most Marwar quartz arenite samples define a general weathering trend sub-parallel to the A-CN boundary (Fig. 13a), consistent with the predicted weathering path, and indicate a limited effect of diagenesis and post-depositional K-metasomatism. Their CIA values (77.8–94.8) are higher than PAAS, indicating moderate to intense weathering in the source area (Fig. 13b). The Nagaur Formation quartz arenites display significantly high CIA values (92.3–94.8) as compared to the Sonia and Girbhakar formations, probably due to strong chemical weathering.

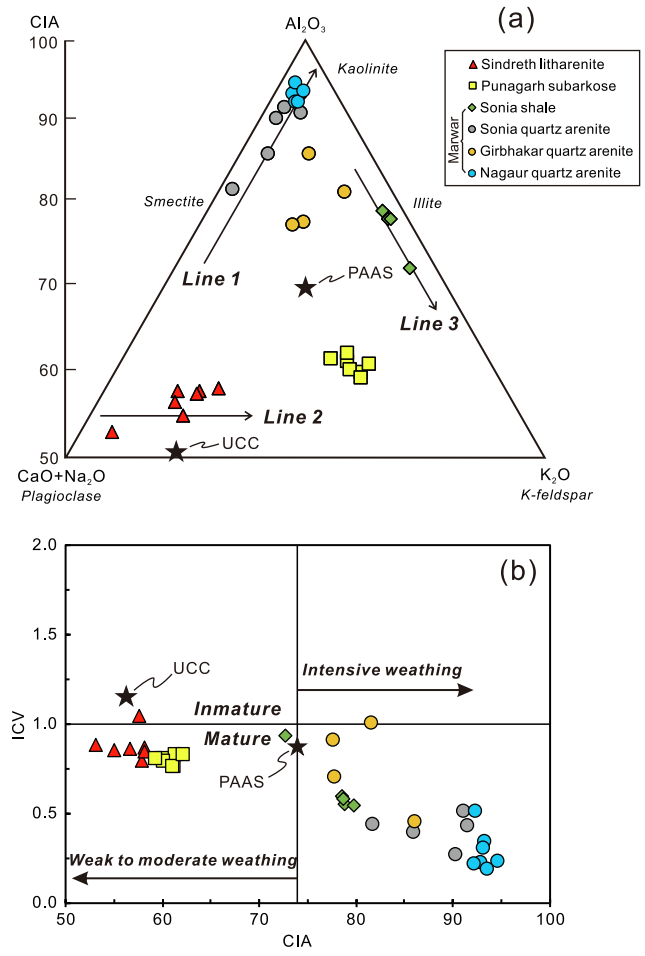

Fig. 13. (a) Chemical Index of Alteration (CIA) Al_2O_3-(CaO^*+Na_2O)-K_2O ternary plots (molecular proportions) showing the weathering trend of the studied rocks (after Nesbitt and Young, 1982, 1984; Fedo et al., 1995); (b) CIA vs. ICV diagram (after Nesbitt and Young, 1984; Cox et al., 1995) to show the maturity and degree of chemical weathering of the studied rocks.

Besides, the ICV values (0.18–1.00) of Marwar samples are significantly lower than the Sindreth and Punagarh groups, indicating that the Marwar detritus may have experienced recycling and/or strong chemical weathering. A wide scatter in ICV values (0.18–1.00) in the Marwar sandstones may indicate a slight change in the source region during the deposition of the Marwar sediments.

The Sonia shales define a trend parallel to the A-K boundary, indicating that kaolinite was replaced by illite during post-deposition K-metasomatism (line 3 of Fig. 13a). Therefore, the highest CIA value of 79.8 and the lowest ICV value of 0.55 of the sample RJW14-114 could represent the primary CIA and ICV characteristics of Sonia shales. Although, relatively lower in intensity as compared to sandstones, the Sonia shales record intense weathering in the source area and recycling of the detritus.

5.3. Tectonic setting of the Punagarh, Sindreth, and Marwar basins

5.3.1. The Punagarh and Sindreth basins

Clastic mineral composition and whole-rock geochemistry of terrigenous clastic rocks can provide the first-order information on the provenance and tectonic setting of sedimentary basins (Ingersoll and Suczek, 1979; Dickinson et al., 1983; Dickinson, 1985; Bhatia and Crook, 1986; Bai et al., 2021). In the Qt-F-L diagram, the Punagarh samples plot in the recycled orogenic field, close to the craton interior field (Fig. 14a). Similarly, the Punagarh samples plot in the quartzose recycled field, close to the boundary with the craton interior field (Fig. 14b). Intermediate quartz (83–86%) and lithic fragment (6–8%) contents but relatively higher feldspar contents (6–9%) of Punagarh samples indicate that the sediments were sourced from a collisional orogen (Dickinson and Suczek, 1979; Dickinson et al., 1983; Dickinson, 1985). However, high La/Y (1.35–1.61) and low Ti/Zr (5.31–7.71) ratios of Punagarh subarkose samples indicate a passive margin setting (Bhatia and Crook, 1986) (Fig. 15a, b), consistent with the inferences drawn from La-Th-Sc and Th-Sc-Zr/10 ternary diagrams (Fig. 15c, d).

The Sindreth samples indicate a recycled orogen affinity in Qt-F-L and Qm-F-Lt diagrams (Fig. 14a, b), except a single litharenite sample that plots in the transitional recycled field (Fig. 14b). A relatively higher abundance of lithic components dominated by volcanic fragments in the Sindreth sandstones hints at a possible subduction-collision setting (Dickinson, 1985). The Sindreth litharenites have high Sc/Cr (0.09–0.56) ratios that closely resemble the sandstones formed in active continental margin setting (Fig. 15a), while they plot away from any of the designated fields in the Ti/Zr vs. La/Sc diagram (Fig. 15b). Besides, the Sindreth litharenites have similarities with sandstones deposited in an active continental margin (Bhatia and Crook, 1986) (Fig. 15c, d). The detrital zircon ages of Sindreth samples are much closer to the depositional age, indicating sedimentation in a tectonically active basin, as sediments from convergent plate margins are expected to contain large

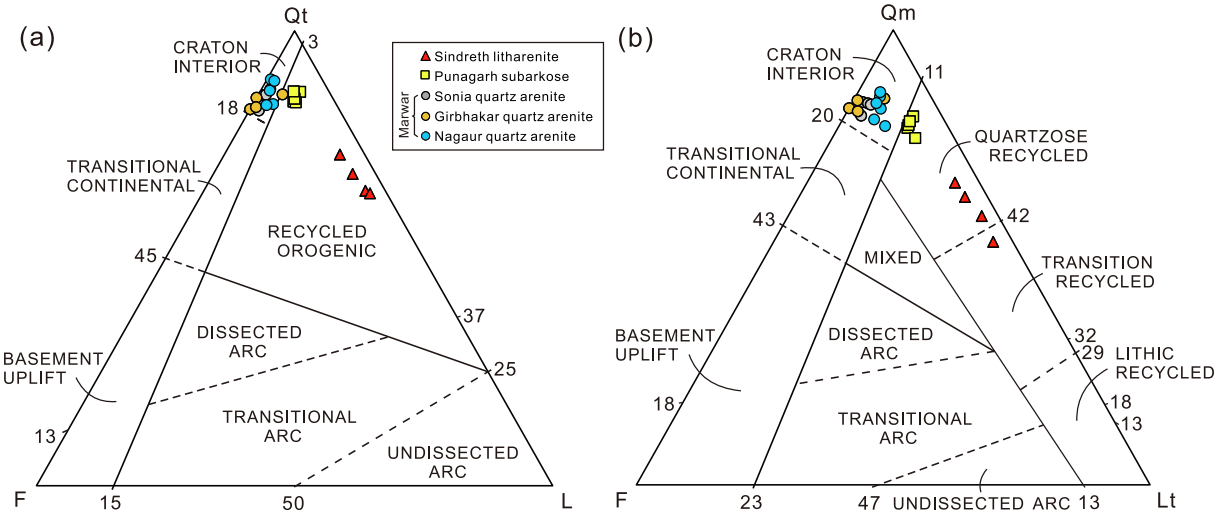

Fig. 14. Ternary plots showing spatially evolutionary variation in sandstone compositions in Sindreth, Punagarh, and Marwar sequences (after Dickinson, 1985).

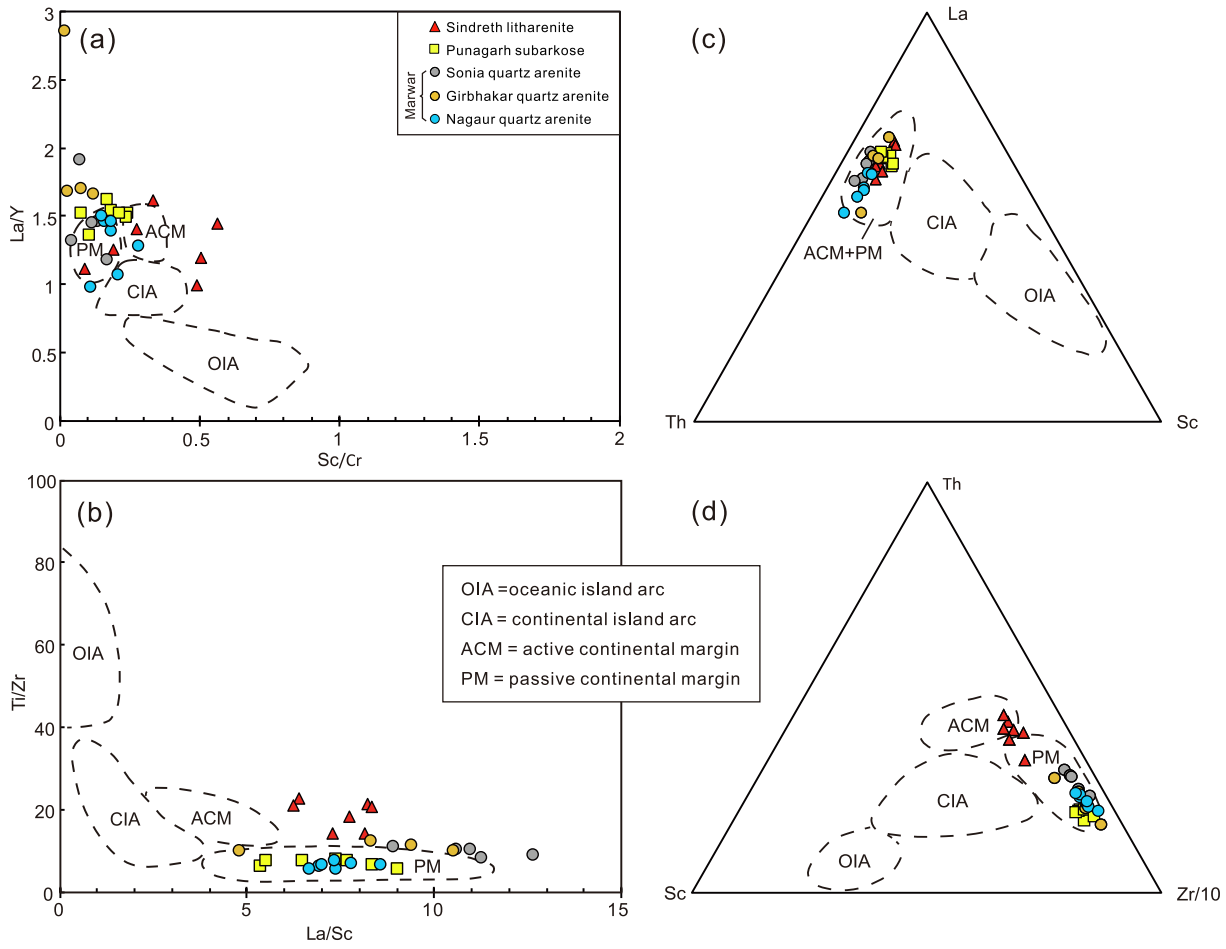

Fig. 15. Tectonic discrimination diagrams of the studied rocks. (a) La/Y-Sc/Cr, (b) Ti/Zr-La/Sc, (c) La-Th-Sc, (d) Th-Sc-Zr/10 ternary diagrams (after Bhatia and Crook, 1986).

proportions of zircon ages close to the depositional age (Cawood et al., 2012). In summary, both compositional and clastic features of Sindreth litharenites point toward deposition in a tectonically active basin.

As discussed in the preceding sections, the Punagarh and Sindreth groups are coeval, however, their provenance and tectonic backgrounds are somewhat different. High ICV values of Punagarh (0.76–0.83) and Sindreth (0.80–1.04) samples indicate immature detritus derived from slightly weathered to unweathered profiles and transport into the sedimentary basin without significant weathering, typical of sedimentation in a tectonically active setting. The Sindreth detrital zircon grains define an age spectrum dominated by Neoproterozoic grains and a minor proportion of Paleoproterozoic to Mesoproterozoic zircons, typical of sediments accumulated in arc setting with sediments derived from the magmatic arc (DeGraaff-Surpless et al., 2002; Cawood et al., 2012). In contrast, a detritus with significantly old components is noted in Punagarh sediments, indicating a cratonic interior source. Such detrital zircon age patterns as well as major and trace elemental compositions of the Punagarh and Sindreth rocks point toward discrete sources, i.e. a cratonic basement and a nearby arc terrane. The bimodal volcaniclastic sequences in the Punagarh and Sindreth basins related to the MIS on account of coeval ages and geochemical similarity (van Lente et al., 2009; de Wall et al., 2012; Dharma Rao et al., 2012; Ashwal et al., 2013) may be useful in understanding the tectonic setting of these two basins. Ashwal et al. (2002) suggest an Andean-type arc setting for the Malani Igneous Suite related to long-lived subduction. The hydrothermally altered basaltic rocks and bimodal magmatism in Sindreth and Punagarh groups further indicate that these two sedimentary sequences were deposited in a back-arc basin (van Lente et al., 2009; Wang et al., 2018c). On the other hand, Schöbel et al. (2017) infer a fault-related continental basin setting for Sindreth bimodal volcanics and clastic sediments. The bimodal volcanism may not necessarily represent continental rift or regional extensional setting related to mantle plume (van Lente et al., 2009; Wang et al., 2018c) and can occur in a back-arc basin, such as the Neoproterozoic bimodal volcanism in the Yangtze Block (Li et al., 2016).

Based on the arguments presented above, we infer that both Punagarh and Sindreth sediments were deposited in an active continental margin setting, such as a back-arc basin, into which both juvenile and old crustal materials were contributed from diverse sources (McLennan et al., 1993), also consistent with Khan and Khan (2015, 2016) and Khan et al. (2020). The Punagarh basin was adjacent to the continental craton and received detritus mainly from an uplifted continental cratonic basement, while the Sindreth basin was close to the magmatic arc and received a dominant volcaniclastic detritus.

5.3.2. *The Marwar basin*

All the Marwar quartz arenite samples plot in the craton interior field in Qt-F-L and Qm-F-Lt diagrams (Fig. 14), indicating sedimentation in a stable continental basin (Dickinson, 1985). Their high Qm/Q ratios (0.94–1) and low feldspar contents affirm a long-distance transport or recycling of older sedimentary/plutonic source rocks (Johnsson, 1993). Nearly all the Marwar quartz arenites plot in the passive continental margin field (Fig. 15), consistent with the significant input of mature detritus in the Marwar sediments relative to the other groups as discussed above. The immature sediments are characteristic of an active continental margin setting, presumably related to an uplifted

continental basement (Bhatia and Crook, 1986). Moreover, relatively lower ICV values (0.18–1.00) of the Marwar samples further indicate a balanced chemical weathering and erosion of the source rocks in a relatively stable tectonic environment. A large number of detrital zircon age peaks obtained for Marwar Supergroup rocks indicate a relatively open sedimentary environment and deposition in a passive continental margin setting with significant detritus input from a large cratonic interior region.

5.4. Geodynamic implications

The tectonic evolution of NW India during the transition from Rodinia to Gondwana continues to be debated, in particular about the diversity in the proposed geodynamics of the Malani Igneous Suite (Eby and Kochhar, 1990; Bhushan, 2000; Torsvik et al., 2001b; Ashwal et al., 2002; Sharma, 2004; Gregory et al., 2009; Meert et al., 2013; Vijaya Rao and Krishna, 2013; Wang et al., 2017b, 2018c; de Wall et al., 2018). Integrating our findings on the Tonian and Cryogenian – early Cambrian Punagarh, Sindreth, and Marwar basins and previous studies, we propose the development of a back-arc basin during the breakup of the Rodinia supercontinent followed by a passive margin during the assembly of the Gondwana supercontinent (Fig. 16). Convergence of the Marwar Block and its subsequent collision with the Aravalli Craton occurred at ~ 1000 Ma (Deb et al., 2001; Pandit et al., 2003). After a quiescence of ~ 100 Ma, the Erinpura Granite emplacement occurred along the western margin of the ADFB, in response to the convergence initiated by the subducting oceanic plate (Just et al., 2011; Solanki, 2011; Wang et al., 2018c). Subsequently, the Punagarh and Sindreth sub-basins opened in a back-arc setting (van Lente et al., 2009; Khan and Khan, 2015, 2016; Wang et al., 2018c; Khan et al., 2020) at ~ 760 Ma, along the western flank of the ADFB (Fig. 16a). The development of a back-arc basin setting for both Punagarh and Sindreth groups has also been proposed in some earlier studies (van Lente et al., 2009; Khan and Khan, 2015, 2016; Wang et al., 2018c; Khan et al., 2020). The presence of E-MORB- and OIB-like basaltic rocks, as well as rhyolites with A_2-subtype granite affinity in the Punagarh and Sindreth basins, point toward a convergent tectonic environment with local extension (e.g. back-arc basin) during the development of these basins (Wang et al., 2017b, 2018c). Moreover, the 770–750 Ma Malani Igneous Suite represents a pulse of magmatic event linking Madagascar, Seychelles, NW India, and South China along the western margin of the Rodinia supercontinent (Zhou et al., 2006; Li et al., 2008; Cawood et al., 2013, 2018; Merdith et al., 2017; Wang et al., 2017b, 2018c). In our proposed model, the Sindreth basin was formed closer to the magmatic arc, while the Punagarh basin was adjacent to the continental craton. At ~ 650 Ma, the Marwar basin opened over the Malani basement, to the west of the Delhi orogenic belt (Vijaya Rao and Krishna, 2013). Consequently, the roughly NNE-SSW trending Marwar Supergroup developed to the west of ADFB in a passive continental margin environment (Fig. 16b). It is noteworthy that several mafic and felsic dykes representing the terminal phase of Malani magmatism in this region intruded both the Punagarh and Sindreth rocks (Chore and Mohanty, 1998; Sharma, 2004; van Lente et al., 2009; Bhardwaj and Biswal, 2019) during the transition from active continental margin setting to passive continental margin setting. The geodynamics during this period remains unclear and needs further attention.

The change in the source area and tectonic setting of the Punagarh, Sindreth, and the overlying Marwar successions can be geodymically linked to the breakup of the Rodinia supercontinent and subsequent assembly of the Gondwana supercontinent. The Indian Block is shown in

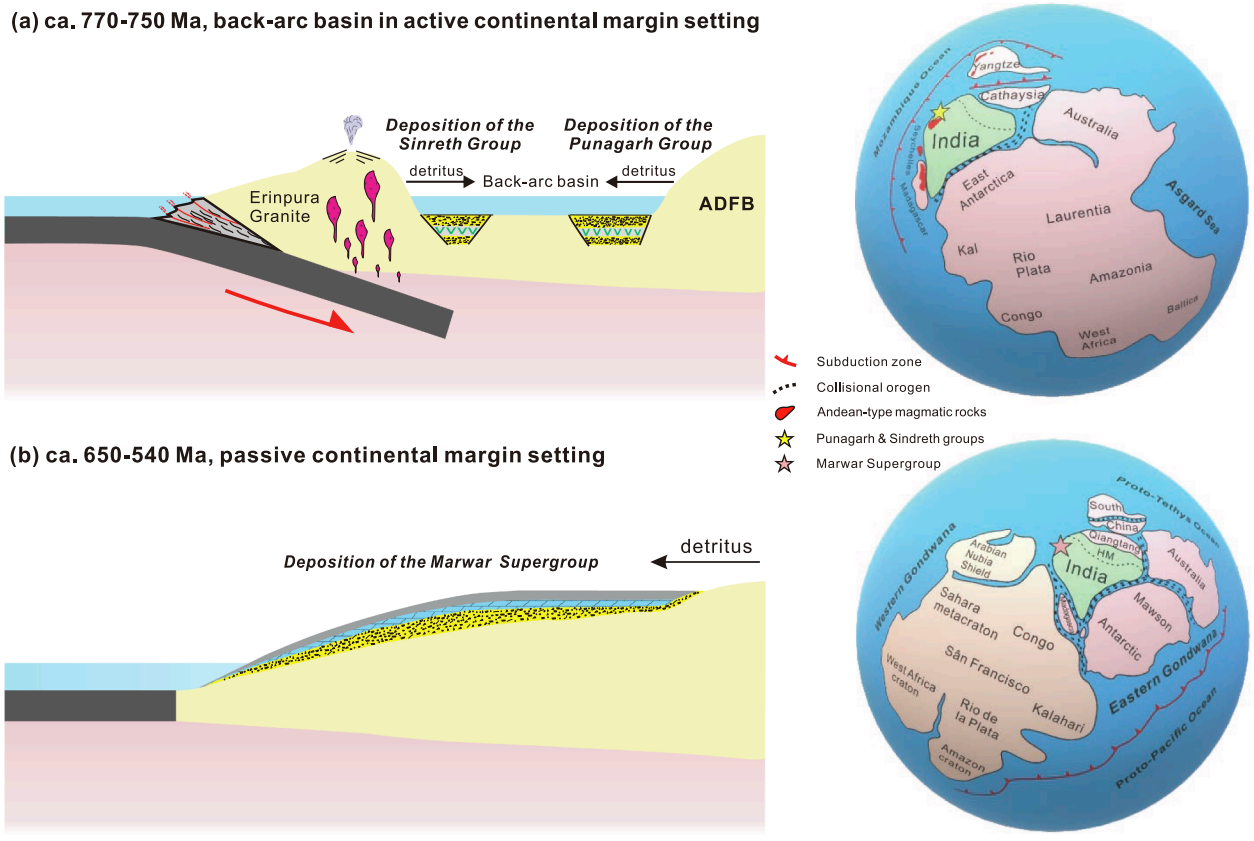

Fig. 16. Cartoon illustrating tectonic evolution of NW India and schematic paleogeographic position of Indian shield during middle Neoproterozoic to early Cambrian (modified from Cawood et al., 2013; Wang et al., 2019). (a) a back-arc basin setting recorded by the Punagarh and Sindreth group rocks indicates an active margin along the western margin of the Rodinia supercontinent during its breakup; (b) a passive continental margin setting recorded by the Marwar Supergroup rocks indicates an open sea between NW Indian and Arabian Nubia Shield along the northern margin of the Gondwana supercontinent during its assembly.

conjugate position with South China, Madagascar, and Seychelles in most of the Rodinia paleogeographic reconstructions, with a subduction-arc accretionary system along the periphery of the Rodinia supercontinent that may be associated with the breakup of the supercontinent (Torsvik et al., 2001a; Meert and Torsvik, 2003; Li et al., 2008; Cawood et al., 2018, 2020; Ranjan et al., 2018) (Fig. 16a; Wang et al., 2021b). This model is consistent with the active continental margin at ~ 760 Ma in NW India recorded by the Punagarh and Sindreth group rocks. During the assembly of the Gondwana, the Indian Block joined with Australia and East Antarctica along the Kunnga-Pinjarra Orogen (Kusky et al., 2003; Meert, 2003; Cawood and Buchan, 2007; Collins et al., 2014; Vadlamani, 2019; Wang et al., 2021b). The East African orogen associated with the assembly of Eastern and Western Gondwana resulted in the amalgamation of southern India, east-central Africa, SW Madagascar, and Sri Lanka (Kröner et al., 1999, 2000, 2003; Collins et al., 2007; Jöns and Schenk, 2008; He et al., 2018) (Fig. 16b). However, in the northern extension of Gondwana, sediments from NW India and the Arabian Nubia Shield were deposited on the opposing passive margins (Wang et al., 2019), precluding any collision between NW Indian and Arabian Nubia Shield along the northern margin of the Gondwana supercontinent. This view is also supported by the geochemical and petrographic data on Marwar basin sedimentary rocks, viz., a passive continental margin setting implying an open sea at the northern extent between the Eastern and Western Gondwana.

6. Conclusions

Based on the geological relationships, sandstone petrography, whole-rock geochemistry, and detrital zircon age data, the principal conclusions of this study are as follows:

(1) The detritus for Punagarh and Sindreth basins were derived from felsic provenance that had undergone moderate to weak chemical weathering. In contrast, the Marwar basin detritus corresponds to a felsic source with moderate to intense chemical weathering.
(2) Punagarh and Sindreth basins are coeval back-arc basins. The Sindreth basin was located close to a magmatic arc and received the detritus with a higher proportion of volcanic rocks while the Punagarh basin was proximal to the continental craton and received predominant detritus supplied from the uplifted continental cratonic basement. In contrast, the Marwar sediments were deposited in a passive continental margin basin with sediments evenly sourced from a large cratonic interior region.
(3) The active continental margin setting recorded by the Punagarh and Sindreth groups corresponds to the peripherical subduction associated with the breakup of the Rodinia supercontinent, while the Marwar Supergroup sediments indicate a passive margin setting and a remnant ocean between NW India and Western Gondwana during the assembly of Gondwana supercontinent.

CRediT authorship contribution statement

Jun Zhang: Investigation, Methodology, Formal analysis, Writing – original draft, Writing – review & editing, Visualization. **Manoj K. Pandit:** Writing – review & editing. **Wei Terry Chen:** Writing – review & editing. **Wei Wang:** Project administration, Supervision, Investigation, Methodology, Resources, Writing – review & editing.

Declaration of Competing Interest

The authors declare that they have no known competing financial interests or personal relationships that could have appeared to influence the work reported in this paper.

Acknowledgments

This study was supported by the National Natural Science Foundation of China (NSFC 41972242 and 41822303) and the Fok Ying Tung Education Foundation (171013). We would like to thank Yin Wei and Liang Li for their help in elemental and isotopic analyses. Vivek Kumar Meena is thanked for his generous help during the fieldwork. Constructive and critical comments from three anonymous reviewers and the editor, Ibrahim Uysal have helped significantly in improving the manuscript.

Appendix A. Supplementary material

Supplementary data to this article can be found online at https://doi.org/10.1016/j.jseaes.2022.105171.

References

Ashwal, L.D., Demaiffe, D., Torsvik, T.H., 2002. Petrogenesis of Neoproterozoic Granitoids and Related Rocks from the Seychelles: the Case for an Andean-type Arc Origin. J. Petrol. 43, 45–83.
Ashwal, L.D., Solanki, A., Pandit, M., Corfu, F., Hendriks, B., Burke, K., Torsvik, T.H., 2013. Geochronology and geochemistry of Neoproterozoic Mt. Abu granitoids, NW India: Regional correlation and implications for Rodinia paleogeography. Precam. Res. 236, 265–281.
Bai, D.-Y., Jiang, Q.-S., Li, B., Jiang, W., Li, Y.-M., 2021. Geochemistry and tectonic implication of the sedimentary rocks in Lengjiaxi Group in northeastern Hunan. Bull. Geol. Sci. Technol. 40 (1), 1–13 in Chinese with English abstract.
Bhardwaj, A., Biswal, T.K., 2019. Deformation and Tectonic History of Punagarh Basin in the Trans-Aravalli Terrane of North-Western India. In: Mondal, M.E.A. (Ed.), Geological Evolution of the Precambrian Indian Shield. Springer International Publishing, Cham, pp. 159–178.
Bhatia, M.R., Crook, K.A.W., 1986. Trace element characteristics of graywackes and tectonic setting discrimination of sedimentary basins. Contrib. Mineral. Petrol. 92, 181–193.
Bhowmik, S.K., Dasgupta, S., 2012. Tectonothermal evolution of the Banded Gneissic Complex in central Rajasthan, NW India: Present status and correlation. J. Asian Earth Sci. 49, 339–348.
Bhushan, S.K., 2000. Malani Rhyolites - A Review. Gondwana Res. 3, 65–77.
Biju-Sekhar, S., Yokoyama, K., Pandit, M.K., Okudaira, T., Yoshida, M., Santosh, M., 2003. Late Paleoproterozoic magmatism in Delhi Fold Belt, NW India and its implication: Evidence from EPMA chemical ages of zircons. J. Asian Earth Sci. 22, 189–207.
Buick, I.S., Allen, C.M., Pandit, M., Rubatto, D., Hermann, J., 2006. The Proterozoic magmatic and metamorphic history of the Banded Gneiss Complex, central Rajasthan, India: LA-ICP-MS U-Pb zircon constraints. Precam. Res. 151, 119–142.
Cawood, P.A., Buchan, C., 2007. Linking accretionary orogenesis with supercontinent assembly. Earth Sci. Rev. 82, 217–256.
Cawood, P.A., Hawkesworth, C.J., Dhuime, B., 2012. Detrital zircon record and tectonic setting. Geology 40, 875–878.
Cawood, P.A., Wang, W., Zhao, T.-Y., Xu, Y.-J., Mulder, J.A., Pisarevsky, S.A., Zhang, L.-M., Gan, C.-S., He, H.-Y., Liu, H.-C., Qi, L., Wang, Y.-J., Yao, J.-L., Zhao, G.-C., Zhou, M.-F., Zi, J.-W., 2020. Deconstructing South China and consequences for reconstructing Nuna and Rodinia. Earth Sci. Rev. 204, 103169.
Cawood, P.A., Wang, Y.-J., Xu, Y.-J., Zhao, G.-C., 2013. Locating South China in Rodinia and Gondwana: A fragment of Greater India Lithosphere? Geology 41, 903–906.
Cawood, P.A., Zhao, G.-C., Yao, J.-L., Wang, W., Xu, Y.-J., Wang, Y.-J., 2018. Reconstructing South China in Phanerozoic and Precambrian supercontinents. Earth Sci. Rev. 186, 173–194.
Chaudhuri, A., Mukhopadhyay, J., Patranabis-Deb, S., Chanda, S.K., 1999. The Neoproterozoic Cratonic Successions of Peninsular India. Gondwana Res. 2, 213–225.
Chauhan, D.S., Mathur, K.M., Ram, N., 2001. Geological nature of the Pokaran Boulder Bed: Palaeoenvironmental, palaeoclimatic and stratigraphic implications. J. Geol. Soc. India 58, 425–433.
Chauhan, D.S., Ram, B., 1999. Ripple marks and synthesis of beach sequences: A study of early Palaeozoic sandstone of Jodhpur Group. Western Rajasthan. Geol. Evol. West. India 66–78.
Chauhan, D.S., Ram, B., Ram, N., 2004. Jodhpur sandstone: A gift of ancient beaches to western Rajasthan. J. Geol. Soc. India 64, 265–276.
Chore, S.A., Mohanty, M., 1998. Stratigraphy and tectonic setting of the Trans-Aravalli neoproterozoic volcanosedimentary sequences in Rajasthan. J. Geol. Soc. India 51, 57–68.
Choudhary, A.K., Gopalan, K., Sastry, C.A., 1984. Present status of the geochronology of the Precambrian rocks of Rajasthan. Tectonophysics 105, 131–140.
Collins, A.S., Clark, C., Plavsa, D., 2014. Peninsular India in Gondwana: The tectonothermal evolution of the Southern Granulite Terrain and its Gondwanan counterparts. Gondwana Res. 25, 190–203.
Collins, A.S., Clark, C., Sajeev, K., Santosh, M., Kelsey, D.E., Hand, M., 2007. Passage through India: the Mozambique Ocean suture, high-pressure granulites and the Palghat-Cauvery shear zone system. Terra Nova 19, 141–147.

Collins, A.S., Pisarevsky, S.A., 2005. Amalgamating eastern Gondwana: The evolution of the Circum-Indian Orogens. Earth Sci. Rev. 71, 229–270.
Condie, K.C., 1993. Chemical composition and evolution of the upper continental crust: Contrasting results from surface samples and shales. Chem. Geol. 104, 1–37.
Coulson, A.L., 1933. The geology of Sirohi state. Rajputana. Mem. Geol. Surv. India 63, 166.
Cox, R., Lowe, D.R., Cullers, R.L., 1995. The influence of sediment recycling and basement composition on evolution of mudrock chemistry in the southwestern United States. Geochim. Cosmochim. Acta 59, 2919–2940.
Cozzi, A., Rea, G., Craig, J., Bhat, G.M., Craig, J., Thurow, J.W., Thusu, B., Cozzi, A., 2012. From global geology to hydrocarbon exploration: Ediacaran-Early Cambrian petroleum plays of India, Pakistan and Oman, Geology and Hydrocarbon Potential of Neoproterozoic-Cambrian Basins in Asia. Geological Society of London 131–162.
de Wall, H., Pandit, M.K., Donhauser, I., Schöbel, S., Wang, W., Sharma, K.K., 2018. Evolution and tectonic setting of the Malani – Nagarparkar Igneous Suite: A Neoproterozoic Silicic-dominated Large Igneous Province in NW India-SE Pakistan. J. Asian Earth Sci. 160.
de Wall, H., Pandit, M.K., Dotzler, R., Just, J., 2012. Cryogenian transpression and granite intrusion along the western margin of Rodinia (Mt. Abu region): Magnetic fabric and geochemical inferences on Neoproterozoic geodynamics of the NW Indian block. Tectonophysics 554–557, 143–158.
Deb, M., Thorpe, R.I., Krstic, D., Corfu, F., Davis, D.W., 2001. Zircon U-Pb and galena Pb isotope evidence for an approximate 1.0 Ga terrane constituting the western margin of the Aravalli-Delhi orogenic belt, northwestern India. Precam. Res. 108, 195–213.
DeGraaff-Surpless, K., Graham, S.A., Wooden, J.L., McWilliams, M.O., 2002. Detrital zircon provenance analysis of the Great Valley Group, California: Evolution of an arc-forearc system. Geol. Soc. Am. Bull. 114, 1564–1580.
Dharma Rao, C.V., Santosh, M., Kim, S.W., 2012. Cryogenian volcanic arc in the NW Indian Shield: Zircon SHRIMP U-Pb geochronology of felsic tuffs and implications for Gondwana assembly. Gondwana Res. 22, 36–53.
Dharma Rao, C.V., Santosh, M., Kim, S.W., Li, S., 2013. Arc magmatism in the Delhi Fold Belt: SHRIMP U-Pb zircon ages of granitoids and implications for Neoproterozoic convergent margin tectonics in NW India. J. Asian Earth Sci. 78, 83–99.
Dickinson, W.R., 1985. Interpreting Provenance Relations from Detrital Modes of Sandstones. In: Zuffa, G.G. (Ed.), Provenance of Arenites. Springer, Netherlands, Dordrecht, pp. 333–361.
Dickinson, W.R., Beard, L.S., Brakenridge, G.R., Erjavec, J.L., Ferguson, R.C., Inman, K. F., Knepp, R.A., Lindberg, F.A., Ryberg, P.T., 1983. Provenance of North American Phanerozoic sandstone in relation to tectonic setting. Geol. Soc. Am. Bull. 94, 222–235.
Dickinson, W.R., Suczek, C.A., 1979. Plate Tectonics and Sandstone Compositions. Am. Assoc. Petrol. Geol. Bull. 63, 2164–2182.
Eby, G.N., Kochhar, N., 1990. Geochemistry and petrogenesis of the Malani igneous suite, North Peninsular India. J. Geol. Soc. India 36, 109–130.
Evans, D., 2013. Reconstructing pre-Pangean supercontinents. Geol. Soc. Am. Bull. 125, 1735–1751.
Fedo, C.M., Nesbitt, H.W., Young, G.M., 1995. Unraveling the effects of potassium metasomatism in sedimentary rocks and paleosols, with implications for paleoweathering conditions and provenance. Geology 23, 921–924.
Floyd, P.A., Leveridge, B.E., 1987. Tectonic environment of the Devonian Gramscatho basin, south Cornwall: framework mode and geochemical evidence from turbiditic sandstones. J. Geol. Soc. 144, 531–542.
Fralick, P.W., Kronberg, B.I., 1997. Geochemical discrimination of clastic sedimentary rock sources. Sediment. Geol. 113, 111–124.
George, B.G., 2020. Geology of the Neoproterozoic – Early Cambrian Marwar Supergroup, Rajasthan: A Synthesis. Proc. Indian Natn. Sci. Acad. 86, 1057–1068.
George, B.G., 2021. On Chhoti Khatu volcanics of Rajasthan and its relationship with the Malani magmatism: A geochemical study. J. Earth Syst. Sci. 130, 74.
George, B.G., Ray, J.S., 2017. Provenance of sediments in the Marwar Supergroup, Rajasthan, India: Implications for basin evolution and Neoproterozoic global events. J. Asian Earth Sci. 147, 254–270.
Gopalan, K., Macdougall, J.D., Roy, A.B., Murali, A.V., 1990. Sm-Nd evidence for 3.3 Ga old rocks in Rajasthan, northwestern India. Precam. Res. 48, 287–297.
Gregory, L.C., Meert, J.G., Bingen, B., Pandit, M.K., Torsvik, T.H., 2009. Paleomagnetism and geochronology of the Malani Igneous Suite, Northwest India: Implications for the configuration of Rodinia and the assembly of Gondwana. Precam. Res. 170, 13–26.
Gupta, B.C., 1934. The geology of central Mewar. Memoir Geological Survey of India 107–168.
Gupta, S.N., Arora, Y.K., Mathur, R.K., Iqballuddin Prasad, B., Sahai, T.N., Sharma, S.B., 1980. Lithostratigraphic map of the Aravalli region. Geological Survey of India, Calcutta, scale 1:1,000,000.
He, X.-F., Hand, M., Santosh, M., Kelsey, D.E., Morrissey, L.J., Tsunogae, T., 2018. Long-lived metamorphic P-T–t evolution of the Highland Complex, Sri Lanka: Insights from mafic granulites. Precam. Res. 316, 227–243.
Heron, A.M., 1953. The geology of Central Rajputana and adjacent districts. Geological Survey of India, p. 389.
Hoffman, P., 1991. Did the Breakout of Laurentia Turn Gondwanaland Inside-Out? Science 252, 1409–1412.
Ingersoll, R.V., Suczek, C.A., 1979. Petrology and provenance of Neogene sand from Nicobar and Bengal Fans, DSDP sites 211 and 218. J. Sediment. Petrol. 49, 1217–1228.
Johnsson, M.J., 1993. The system controlling the composition of clastic sediments, In: Johnsson, M.J., Basu, A. (Eds.), Processes Controlling the Composition of Clastic Sediments. Geological Society of America, pp. 1-20.
Jöns, N., Schenk, V., 2008. Relics of the Mozambique Ocean in the central East African Orogen: evidence from the Vohibory Block of southern Madagascar. J. Metamorphic Geol. 26, 17–28.
Just, J., Schulz, B., de Wall, H., Jourdan, F., Pandit, M.K., 2011. Monazite CHIME/EPMA dating of Erinpura granitoid deformation: Implications for Neoproterozoic tectono-thermal evolution of NW India. Gondwana Res. 19, 402–412.
Kaur, P., Chaudhri, N., Raczek, I., Kröner, A., Hofmann, A., Okrusch, M., 2011. Zircon ages of late Palaeoproterozoic (ca. 1.72–1.70Ga) extension-related granitoids in NE Rajasthan, India: Regional and tectonic significance. Gondwana Res. 19, 1040–1053.
Kaur, P., Zeh, A., Chaudhri, N., 2017. Palaeoproterozoic continental arc magmatism, and Neoproterozoic metamorphism in the Aravalli-Delhi orogenic belt, NW India: New constraints from in situ zircon U-Pb-Hf isotope systematics, monazite dating and whole-rock geochemistry. J. Asian Earth Sci. 136, 68–88.
Kaur, P., Zeh, A., Chaudhri, N., 2021. Archean to Proterozoic (3535–900 Ma) crustal evolution of the central Aravalli Banded Gneissic Complex, NW India: New constraints from zircon U-Pb-Hf isotopes and geochemistry. Precam. Res. 359, 106179.
Kaur, P., Zeh, A., Chaudhri, N., Gerdes, A., Okrusch, M., 2013. Nature of magmatism and sedimentation at a Columbia active margin: Insights from combined U-Pb and Lu–Hf isotope data of detrital zircons from NW India. Gondwana Res. 23, 1040–1052.
Khan, M.S., Irshad, R., Khan, T., 2019. Geochemistry of Mafic-Felsic Rocks of Phulad Ophiolite, in and Around Pindwara-Mount Abu Region, South Delhi Fold Belt, NW Indian Shield: Implications for Its Tectonic Evolution. In: Mondal, M.E.A. (Ed.), Geological Evolution of the Precambrian Indian Shield. Springer International Publishing, Cham, pp. 401–441.
Khan, M.S., Smith, T.E., Raza, M., Huang, J., 2005. Geology, Geochemistry and Tectonic Significance of Mafic-ultramafic Rocks of Mesoproterozoic Phulad Ophiolite Suite of South Delhi Fold Belt. NW Indian Shield. Gondwana Res. 8, 553–566.
Khan, T., Khan, M.S., 2015. Clastic rock geochemistry of Punagarh basin, trans-Aravalli region, NW Indian shield: implications for paleoweathering, provenance, and tectonic setting. Arabian J. Geosci. 8, 3621–3644.
Khan, T., Khan, M.S., 2016. Geochemistry of the sandstones of Punagarh basin: Implications for two source terranes and Arabian - Nubian connection of Aravalli craton? J. Geol. Soc. India 88, 366–386.
Khan, T., Sarma, D.S., Khan, M.S., 2020. Geochemical study of the Neoproterozoic clastic sedimentary rocks of the Khambal Formation (Sindreth Basin), Aravalli Craton, NW Indian Shield: Implications for paleoweathering, provenance, and geodynamic evolution. Geochemistry 80, 125596.
Kröner, A., Hegner, E., Collins, A., Windley, B.F., Brewer, T.S., Razakamanana, T., Pidgeon, R., 2000. Age and magmatic history of the Antananarivo block, central Madagascar, as derived from zircon geochronology and Nd isotopic systematics. Am. J. Sci. 300, 251–288.
Kröner, A., Muhongo, S., Hegner, E., Wingate, M.T.D., 2003. Single-zircon geochronology and Nd isotopic systematics of Proterozoic high-grade rocks from the Mozambique belt of southern Tanzania (Masasi area): Implications for Gondwana assembly. J. Geol. Soc. 160, 745–757.
Kröner, A., Windley, B.F., Jaeckel, P., Brewer, T.S., Razakamanana, T., 1999. New zircon ages and regional significance for the evolution of the Pan-African orogen in Madagascar. J. Geol. Soc. 156, 1125–1135.
Kumar, S., Pandey, S.K., 2008. Discovery of trilobite trace fossils from the Nagaur Sandstone, the Marwar Supergroup, Dulmera area, Bikaner District. Rajasthan. Curr. Sci. 94, 1081–1085.
Kumar, S., Pandey, S.K., 2010. Trace fossils from the Nagaur Sandstone, Marwar Supergroup, Dulmera area, Bikaner district, Rajasthan. India. J. Asian Earth Sci. 38, 77–85.
Kusky, T.M., Abdelsalam, M., Tucker, R.D., Stern, R.J., 2003. Evolution of the East African and related orogens, and the assembly of Gondwana. Precam. Res. 123, 81–85.
Lan, Z., Zhang, S., Li, X.-H., Pandey, S.K., Sharma, M., Shukla, Y., Ahmad, S., Sarkar, S., Zhai, M., 2020. Towards resolving the 'jigsaw puzzle' and age-fossil inconsistency within East Gondwana. Precam. Res. 345, 105775.
Li, L.-M., Lin, S.-F., Xing, G.-F., Davis, D.W., Jiang, Y., Davis, W., Zhang, Y.-J., 2016. Ca. 830Ma back-arc type volcanic rocks in the eastern part of the Jiangnan orogen: Implications for the Neoproterozoic tectonic evolution of South China Block. Precam. Res. 275, 209–224.
Li, Z.-X., Bogdanova, S.V., Collins, A.S., Davidson, A., De Waele, B., Ernst, R., Fitzsimons, I., Fuck, R.A., Gladkochub, D.P., Jacobs, J., Karlstrom, K., Sn, L., Natapov, L.M., Pease, V., Pisarevsky, S., Thrane, K., Vernikovsky, V., 2008. Assembly, configuration, and break-up history of Rodinia: A synthesis. Precam. Res. 160, 179–210.
Malone, S., Meert, J., Banerjee, D., Pandit, M., Tamrat, E., Kamenov, G., Pradhan, V., Sohl, L., 2008. Paleomagnetism and Detrital Zircon Geochronology of the Upper Vindhyan Sequence, Son Valley and Rajasthan, India: A ca. 1000Ma Closure age for the Purana Basins? Precam. Res. 164, 137–159.
Manikyamba, C., Ganguly, S., Pahari, A., 2021. Geochemical Features of Bellara Trap Volcanic Rocks of Chitradurga Greenstone Belt, Western Dharwar Craton, India: Insights into MORB-BABB Association from a Neoarchean Back-Arc Basin. J. Earth Sci. 32, 1528–1544.
Mazumdar, A., Bhattacharya, S.K., 2004. Stable isotopic study of late neoproterozoic-early Cambrian (?) sediments from Nagaur-Ganganagar basin, western India: Possible signatures of global and regional C-isotopic events. Geochem. J. 38, 163–175.
McBride, E.F., 1963. A Classification of Common Sandstones. J. Sediment. Res. 33.
McKenzie, N.R., Hughes, N.C., Myrow, P.M., Xiao, S., Sharma, M., 2011. Correlation of Precambrian-Cambrian sedimentary successions across northern India and the utility

of isotopic signatures of Himalayan lithotectonic zones. Earth Planet. Sci. Lett. 312, 471–483.
McLennan, S.M., Hemming, S., McDaniel, D., Hanson, G., 1993. Geochemical approaches to sedimentation, provenance, and tectonics. In: Johnsson, M.J., Basu, A. (Eds.), Processes Controlling the Composition of Clastic Sediments. Geological Society of America, pp. 21–40.
Meert, J.G., 2003. A synopsis of events related to the assembly of eastern Gondwana. Tectonophysics 362, 1–40.
Meert, J.G., Pandit, M.K., Pradhan, V., Banks, J., Sirianni, R., Stroud, M., Newstead, B., Gifford, J., 2010. Precambrian crustal evolution of Peninsular India: A 3.0 billion year odyssey. J. Asian Earth Sci. 39, 483–515.
Meert, J.G., Pandit, M.K., Kamenov, G.D., 2013. Further geochronological and paleomagnetic constraints on Malani (and pre-Malani) magmatism in NW India. Tectonophysics 608, 1254–1267.
Meert, J.G., Torsvik, T.H., 2003. The making and unmaking of a supercontinent: Rodinia revisited. Tectonophysics 375, 261–288.
Merdith, A., Collins, A., Williams, S., Pisarevsky, S., Foden, J., Archibald, D., Blades, M., Alessio, B., Armistead, S., Zivak, D., Clark, C., Müller, D., 2017. A full-plate global reconstruction of the Neoproterozoic. Gondwana Res. 50, 84–134.
Moores, E., 1991. Southwest U.S.-East Antarctica (SWEAT) connection: A hypothesis. Geology 19, 425–428.
Nance, R.D., Murphy, J.B., Santosh, M., 2014. The supercontinent cycle: A retrospective essay. Gondwana Res. 25, 4–29.
Naqvi, S.M., 2005. Geology and evolution of the Indian plate: From Hadean to Holocene, 4 Ga to 4 Ka. Capital Publishing Company, New Delhi, India.
Nesbitt, H.W., Young, G.M., 1982. Early Proterozoic climates and plate motions inferred from major element chemistry of lutites. Nature 299, 715–717.
Nesbitt, H.W., Young, G.M., 1984. Prediction of some weathering trends of plutonic and volcanic rocks based on thermodynamic and kinetic considerations. Geochim. Cosmochim. Acta 48, 1523–1534.
Pandey, D.K., Bahadur, T., 2009. A review of the stratigraphy of Marwar Supergroup of west-central Rajasthan. J. Geol. Soc. India 73, 747–758.
Pandit, M.K., Carter, L.M., Ashwal, L.D., Tucker, R.D., Torsvik, T.H., Jamtveit, B., Bhushan, S.K., 2003. Age, petrogenesis and significance of 1Ga granitoids and related rocks from the Sendra area, Aravalli Craton. NW India. J. Asian Earth Sci. 22, 363–381.
Pandit, M.K., Kumar, H., Wang, W., 2021. Geochemistry and geochronology of A-type basement granitoids in the north-central Aravalli Craton: Implications on Paleoproterozoic geodynamics of NW Indian Block. Geosci. Front. 12, 101084.
Pandit, M.K., Sial, A.N., Jamrani, S.S., Ferreira, V.P., 2001. Carbon Isotopic Profile Across the Bilara Group Rocks of Trans-Aravalli Marwar Supergroup in Western India: Implications for Neoproterozoic — Cambrian Transition. Gondwana Res. 4, 387–394.
Pareek, H.S., 1981. Petrochemistry and Petrogenesis of the Malani Igneous Suite. India. Geol. Soc. Am. Bull. 92, 206–273.
Pareek, H.S., 1984. Pre-Quaternary geology and mineral resources of northwestern Rajasthan. Memoir Geological Survey of India 1–99.
Purohit, R., Papineau, D., Kröner, A., Sharma, K.K., Roy, A.B., 2012. Carbon isotope geochemistry and geochronological constraints of the Neoproterozoic Sirohi Group from northwest India. Precam. Res. 220–221, 80–90.
Ranjan, S., Upadhyay, D., Abhinay, K., Pruseth, K.L., Nanda, J.K., 2018. Zircon geochronology of deformed alkaline rocks along the Eastern Ghats Belt margin: India-Antarctica connection and the Enderbia continent. Precam. Res. 310, 407–424.
Roy, A.B., Jakhar, S.R., 2002. Geology of Rajasthan (Northwest India) - Precambrian to Recent. Scientific Publishers (India), Jodhpur.
Roy, A.B., Kröner, A., 1996. Single zircon evaporation ages constraining the growth of the Archaean Aravalli craton, northwestern Indian shield. Geol. Mag. 133, 333–342.
Roy, A.B., Sharma, K.K., 1999. Geology of the region around Sirohi Town, Western Rajasthan-Story of Neoproterozoic evolution of the Trans-Aravalli crust. In: Paliwal, B.S. (Ed.), Geological Evolution of NW Indian Crust. Scientific Publishers (India), Jodhpur, pp. 19–33.
Saini, P., Singh, S., Pandit, M.K., 2006. Angular relationship between rocks of the Aravalli and Delhi Supergroups in southeastern Rajasthan - A possible unconformity. Curr. Sci. 91, 432–434.
Schöbel, S., Sharma, K., Hörbrand, T., Böhm, T., Donhauser, I., de Wall, H., 2017. Continental rift-setting and evolution of Neoproterozoic Sindreth Basin in NW-India. J. Earth Syst. Sci. 126.
Sharma, K.K., 2004. The Neoproterozoic Malani magmatism of the northwestern Indian shield: Implications for crust-building processes. J. Earth Syst. Sci. 113, 795–807.
Sharma, K.K., 2005. Malani magmatism: An extensional lithospheric tectonic origin, Plates, plumes and paradigms. Geological Society of America 463–476.
Singh, V.K., Babu, R., Kumar, P., Shukla, M., 2008. Ediacaran-Phanerozoic fossils assemblage from the Marwar Supergroup, Western Rajasthan, India. In: Yanko Hombach, V. (Ed.), Proceeding of 5th International Conference on Environmental Micropaleontology, Microbiology and Meiobenthology. University of Madras, India, pp. 291–294.
Sinha-Roy, 1984. Precambrian crustal interaction in Rajasthan, NW India, Proceedings of the seminar on Crustal Evolution of Indian Shield and its Bearing on Metallogeny. Indian Journal of Earth Sciences, pp. 84-91.
Sinha-Roy, S., Malhotra, G., Mohanty, M., 1998. Geology of Rajasthan. Geological Society of India, Bangalore, India, p. 278.
Solanki, A.M., 2011. A petrographic, geochemical and geochronological investigation of deformed granitoids from SW Rajasthan: Neoproterozoic age of formation and evidence of Pan-African imprint. University of the Witwatersrand Johannesburg.
Srivastava, P., 2012. Treptichnus pedum: An Ichnofossil Representing Ediacaran - Cambrian Boundary in the Nagaur Group, the Marwar Supergroup, Rajasthan. India. Proc. Indian Natn. Sci. Acad. 78, 161–169.
Taylor, S.R., McLennan, S.M., 1985. The Continental Crust: its Composition and Evolution, An Examination of the Geochemical Record Preserved in Sedimentary Rocks. Oxford Blackwell.
Tobisch, O.T., Collerson, K.D., Bhattacharyya, T., Mukhopadhyay, D., 1994. Structural relationships and Sr-Nd isotope systematics of polymetamorphic granitic gneisses and granitic rocks from central Rajasthan, India: implications for the evolution of the Aravalli craton. Precam. Res. 65, 319–339.
Torsvik, T.H., Ashwal, L.D., Tucker, R.D., Eide, E.A., 2001a. Neoproterozoic geochronology and palaeogeography of the Seychelles microcontinent: the India link. Precam. Res. 110, 47–59.
Torsvik, T.H., Carter, L.M., Ashwal, L.D., Bhushan, S.K., Pandit, M.K., Jamtveit, B., 2001b. Rodinia refined or obscured: Palaeomagnetism of the Malani Igneous Suite (NW India). Precam. Res. 108, 319–333.
Turner, C.C., Meert, J.G., Pandit, M.K., Kamenov, G.D., 2014. A detrital zircon U-Pb and Hf isotopic transect across the Son Valley sector of the Vindhyan Basin, India: Implications for basin evolution and paleogeography. Gondwana Res. 26, 348–364.
Vadlamani, R., 2019. Cambrian Garnet Sm-Nd Isotopic Ages from the Polydeformed Bolangir Anorthosite Complex, Eastern Ghats Belt, India: Implications for Intraplate Orogeny Coeval with Kuunga Orogeny during Gondwana Assembly. J. Geol. 127, 437–456.
van Lente, B., Ashwal, L.D., Pandit, M.K., Bowring, S.A., Torsvik, T.H., 2009. Neoproterozoic hydrothermally altered basaltic rocks from Rajasthan, northwest India: Implications for late Precambrian tectonic evolution of the Aravalli Craton. Precam. Res. 170, 202–222.
Vijaya Rao, V., Krishna, V.G., 2013. Evidence for the Neoproterozoic Phulad Suture Zone and Genesis of Malani magmatism in the NW India from deep seismic images: Implications for assembly and breakup of the Rodinia. Tectonophysics 589, 172–185.
Wang, W., Cawood, P.A., Pandit, M.K., 2021a. India in the Nuna to Gondwana supercontinent cycles: Clues from the north Indian and Marwar Blocks. Am. J. Sci. 321, 83–117.
Wang, W., Cawood, P.A., Pandit, M.K., Xia, X.-P., Raveggi, M., Zhao, J.-H., Zheng, J.-P., Qi, L., 2021b. Fragmentation of South China from greater India during the Rodinia-Gondwana transition. Geology 49, 228–232.
Wang, W., Cawood, P.A., Pandit, M.K., Xia, X.-P., Zhao, J.-H., 2018a. Coupled Precambrian crustal evolution and supercontinent cycles: Insights from in-situ U-Pb, O- and Hf-isotopes in detrital zircon, NW india. Am. J. Sci. 318, 989–1017.
Wang, W., Cawood, P.A., Pandit, M.K., Zhao, J.-H., Zheng, J.-P., 2019. No collision between Eastern and Western Gondwana at their northern extent. Geology 47, 308–312.
Wang, W., Cawood, P.A., Pandit, M.K., Zhou, M.-F., Chen, W.-T., 2017a. Zircon U-Pb age and Hf isotope evidence for an Eoarchaean crustal remnant and episodic crustal reworking in response to supercontinent cycles in NW India. J. Geol. Soc. 174, 759–772.
Wang, W., Cawood, P.A., Pandit, M.K., Zhou, M.-F., Zhao, J.-H., 2018b. Evolving passive- and active-margin tectonics of the Paleoproterozoic Aravalli Basin, NW India. Geol. Soc. Am. Bull. 131, 426–443.
Wang, W., Cawood, P.A., Zhou, M.-F., Pandit, M.K., Xia, X.-P., Zhao, J.-H., 2017b. Low-$\delta^{18}O$ Rhyolites From the Malani Igneous Suite: A Positive Test for South China and NW India Linkage in Rodinia. Geophys. Res. Lett. 44, 10298–210305.
Wang, W., Pandit, M.K., Zhao, J.-H., Chen, W.-T., Zheng, J.-P., 2018c. Slab break-off triggered lithosphere - asthenosphere interaction at a convergent margin: The Neoproterozoic bimodal magmatism in NW India. Lithos 296–299, 281–296.
Wang, X.-C., Wilde, S.A., Li, Z.-X., Li, S.-J., Li, L.-L., 2020. Do Supercontinent-Superplume Cycles Control the Growth and Evolution of Continental Crust? J. Earth Sci. 31, 1142–1169.
Weis, D., Kieffer, B., Maerschalk, C., Barling, J., De Jong, J., Williams, G., Hanano, D., Pretorius, W., Mattielli, N., Scoates, J., Goolaerts, A., Friedman, R., Mahoney, J., 2006. High-precision isotopic characterization of USGS reference materials by TIMS and MC-ICP-MS. Geochem. Geophys. Geosyst. 7.
Wiedenbeck, M., Goswami, J.N., 1994. High precision $^{207}Pb/^{206}Pb$ zircon geochronology using a small ion microprobe. Geochim. Cosmochim. Acta 58, 2135–2141.
Wiedenbeck, M., Goswami, J.N., Roy, A.B., 1996. Stabilization of the Aravalli Craton of northwestern India at 2.5 Ga: An ion microprobe zircon study. Chem. Geol. 129, 325–340.
Xu, H.-R., Meert, J.G., Pandit, M.K., 2022. Age of the Marwar Supergroup, NW India: A note on the U-Pb geochronology of Jodhpur Group felsic volcanics. Geosci. Front. 13, 101287.
Zhao, J.-H., Pandit, M.K., Wang, W., Xia, X.-P., 2018. Neoproterozoic tectonothermal evolution of NW India: Evidence from geochemistry and geochronology of granitoids. Lithos 316–317, 330–346.
Zhao, K., Du, X.-B., Jia, J.-X., Yang, P., Zhang, C., Peng, W., 2020. Provenance analysis of the Pinghu slope belt in Xihu Depression: Evidence from detrital zircon U-Pb chronology and heavy minerals. Bull. Geol. Sci. Technol. 39 (3), 68–76 in Chinese with English abstract.
Zhou, M.-F., Yan, D.-P., Wang, C.-L., Qi, L., Kennedy, A., 2006. Subduction-related origin of the 750 Ma Xuelongbao adakitic complex (Sichuan Province, China): Implications for the tectonic setting of the giant Neoproterozoic magmatic event in South China. Earth Planet. Sci. Lett. 248, 286–300.
Zhou, X., Zheng, J.-P., Li, Y.-B., Griffin, W.L., Xiong, Q., Moghadam, H.S., O'Reilly, S.Y., 2019. Neoproterozoic sedimentary rocks track the location of the Lhasa Block during the Rodinia breakup. Precam. Res. 320, 63–77.